UNIVERSIDADE DA BEIRA INTERIOR
Ciências da Saúde

miR-9 and miR-29 in Alzheimer's disease: assessment of a possible synergy

Joana Filipa Soares Rodrigues

Dissertação para obtenção do Grau de Mestre em
Ciências Biomédicas
(2º ciclo de estudos)

Orientador: Profª. Doutora Fani Sousa
Co-orientador: Doutora Patrícia Pereira

Covilhã, outubro de 2016

Caprice no. 24 in A minor
Niccolò Paganini

To Humanity...

Agradecimentos

Em primeiro lugar, gostaria de agradecer aos Professores que me acompanharam ao longo de todo este processo, nomeadamente à minha Professora Orientadora Doutora Fani Sousa por todo o conhecimento e sugestões partilhados, assim como pelo tempo que me dedicou. Obrigada pela oportuindade. Devo também um agradecimento muito especial à minha Professora Co-orientadora Doutora Patrícia Pereira pelo extenso conhecimento, experiência e boa disposição transmitidos. Muito obrigada pela infindável disponibilidade e paciência demonstradas.

Gostaria também de agradecer ao Professor Doutor João Queiroz, ao Centro de Investigação em Ciências da Saúde e à Faculdade de Ciências da Saúde da Universidade da Beira Interior pela garantia da continuidade do desenvolvimento do projeto através do financiamento destinado ao aprovisionamento de todo o material necessário à correcta dinâmica no espaço laboratorial.

Sinto-me grata à colega Mestre Eduarda Coutinho pelo apoio prestado no importante trabalho de sequenciação nucleotídica. Gostaria também de agradecer ao Doutor Augusto Pedro pela ajuda no processo de quantificação proteica de amostras. Agradeço também a todo o grupo de Biotecnologia e Ciências Biomoleculares, assim como a todos os amigos e colegas investigadores integrantes do CICS que direta ou indiretamente colaboraram no desenvolvimento deste trabalho.

Somos o que vivemos, e a minha felicidade devo-a aos meus eternos heróis, os meus insubstituíveis pai e mãe, António e Lúcia, que me incutiram o amor, a humanidade, a esperança e a fé. Obrigada por tanto, obrigada pela vida. Amo-vos imensuravelmente.

À minha linda irmã Miriam: obrigada por preencheres todos os recantos da minha vida de brilho. Obrigada por fazeres com que a vida tenha um sentido tão lindo assim. Amo-te tanto Mimi.

Um enorme obrigada à minha maravilhosa grande família que tanto contribuiu para o meu crescimento. Muito obrigada por tudo o que lutaram por mim e por outros, muito obrigada pelas memórias vivas reconfortantes, pela inspiração e oportunidades, pelo mundo interior de beleza estonteante que me permitiram criar. Amo-vos família.

O amor floresce em corações lindos, obrigada Ivo Gabriel pela amizade sincera, paciência inabalável e cumplicidade de irmão. Há tanto a viver meu amor...

Meus amigos tão, tão lindos, persistentes, íntimos, autênticos: continuem a sê-lo. Os amigos são a família que se escolhe. Eu escolhi-a muito bem. Obrigada por mim. Amo-vos.

Resumo Alargado

A doença de Alzheimer (DA) tem vindo a tornar-se uma patologia cada vez mais prepoderante principalmente entre idosos. Esta doença é a forma de demência mais prevalente, sendo responsável por 50-70% dos casos. O número de casos de DA por país é muito variável, no entanto, os países da Europa Ocidental são os que mais casos apresentam. Esta é uma doença extremamente incapacitante que leva à perda de funções cerebrais e, consequentemente, a limitações a nível físico, podendo em última instância levar à morte. Ao nível biológico, e em particular na célula, uma das alterações associadas à doença é a elevada produção de péptidos β-amilóide (Aβ) na via amiloidogénica. Esta via celular envolve a clivagem da proteína precursora amilóide (PPA), constituinte de membranas celulares nervosas, pelas β-secretase (BACE1) e γ-secretase. Como tal, é realmente necessária uma intervenção tendo em vista o tratamento da DA procurando reverter a sua etiologia. Uma das vertentes terapêuticas em grande evolução é a terapia génica que se baseia na alteração ou correção da informação genética de um determinado organismo. Neste sentido os microRNAs (miRNAs) têm sido alvo de intensa pesquisa e investigação, uma vez que têm funções de regulação da expressão génica ao nível transcricional, mediante a clivagem ou inibição da tradução de RNA mensageiro (RNAm). Esta propriedade pode ser explorada e aplicada a RNAm que codificam proteínas de interesse. Já foram publicados alguns estudos que descrevem a associação entre dois miRNAs, o miR-9 e miR-29, e duas proteínas envolvidas na via amiloidogénica, nomeadamente a enzima BACE1 e a Presenilina (PSEN). A BACE1 é uma enzima que cliva a PPA e a presenilina (PSEN) é uma proteína necessária à correta actividade da γ-secretase que por sua vez também cliva a PPA. A DA é principalmente causada pela acumulação de péptidos β-amilóides resultantes da acção das enzimas BACE1 e PSEN, formando a placa amilóide no cérebro e danificando os tecidos cerebrais envolventes.

Recentemente, o nosso grupo de investigação comprovou o efeito do microRNA 29 (miR-29) na inibição da expressão da BACE1 em células N2a695 transfectadas com este miRNA. Desta forma, o principal objectivo desta dissertação consiste no estudo do efeito do miR-9 produzido de forma recombinante nos níveis de expressão das proteínas BACE1 e PSEN, bem como a avaliação de uma possível sinergia entre o miR-9 e o miR-29. Efetivamente, os ácidos nucleicos em questão foram transfectados na sua forma não madura, ou seja, como pre-microRNAs (pre-miRs), pre-miR-9 e pre-miR-29, pois após a sua entrada na célula estes precursores são identificados, processados e exercem a sua função.

Os pre-miR-9 e pre-miR-29 foram produzidos de forma recombinante utilizando como hospedeiro *Escherichia coli (E. coli) DH5a* transformada com o plasmídeo pBHSR1-RM. Estas bactérias foram escolhidas porque têm um rápido crescimento e a produção das moléculas de interesse acompanha-o. É de notar que a produção recombinante de biomoléculas neste hospedeiro é vantajosa pois permite a obtenção de diversos produtos de interesse, em

grandes quantidades, sendo rentável do ponto de vista económico. Neste âmbito, torna-se também importante estudar quer os perfis de crescimento da bactéria ao longo do tempo quer os perfis de produção dos miRNAs de forma a identificar o momento em que a produção é maximizada. Paralelamente, a quantidade de ADN genómico (ADNg) bem como o conteúdo proteico são também avaliados ao longo do tempo de crescimento da *E. coli DH5a*. Relativamente ao crescimento da *E. coli DH5a* verificou-se um aumento exponencial até 6 horas após o início da sua fermentação. Verificou-se igualmente que o conteúdo de pre-miR-29 e proteínas acompanhou o crescimento bacteriano, aumentando paralelamente até respetivamente 6 horas e 5 horas após o início da cultura. Por outro lado, os níveis de ADNg aumentaram substancialmente a partir de 6 horas de fermentação. Após a recuperação dos RNAs, é extremamente importante proceder à sua purificação. De facto, considerando a sua potencial aplicação terapêutica, os RNAs devem ser recuperados com elevado grau de pureza, estabilidade e atividade. Neste trabalho, a etapa de purificação foi realizada com recurso à cromatografia de afinidade com arginina imobilizada, visto que estudos anteriores indicaram que a arginina possui caraterísticas que a tornam adequada para a purificação de biomoléculas como o RNA, devido às interações que são estabelecidas. Relativamente ao suporte usado para imobilização do ligando, foi selecionado um suporte monolítico visto que apresenta diversas vantagens, tais como a redução do tempo de corrida, a maior capacidade de ligação, excelentes propriedades de transferência de massa e boa recuperação da amostra. Os suportes monolíticos apresentam também a vantagem de permitirem trabalhar a fluxos superiores e em diferentes escalas. A estratégia estabelecida para a purificação dos pre-miRNAs foi baseada na eluição em condições que promovem preferencialmente interações eletroestáticas, nomeadamente, com aplicação de um gradiente crescente de NaCl em 10 mM Tris-HCl a pH 6.5. Estabeleceram-se dois gradientes distintos para a purificação de cada um dos RNAs, um contendo dois passos de eluição e outro com três passos de eluição. As concentrações definidas para a purificação do pre-miR-29 no primeiro gradiente (de 3 passos) foram 0,94 M NaCl, 1,12 M NaCl e 1,6 M NaCl em 10 mM Tris-HCl a pH 6.5; e no gradiente com 2 passos foram usadas as concentrações de 1 M NaCl e 1,6 M NaCl em 10 mM Tris-HCl a pH 6.5. No caso da purificação do pre-miR-9, as concentrações usadas no gradiente de 3 passos foram de 0,98 M NaCl, 1,12 M NaCl e 1,62 M NaCl em 10 mM Tris-HCl a pH 6.5, ou de 1 M NaCl e 1,6 M NaCl em 10 mM Tris-HCl a pH 6.5, no gradiente de 2 passos. É de notar que apesar de ambos os métodos permitirem a purificação dos pre-miRNAs, a recuperação do pre-miR-9 foi superior no método de dois passos, minimizando desta forma as perdas do RNA de interesse. Já para purificar o pre-miR-29, a estratégia de três passos revelou-se mais adequada. Os ácidos nucleicos purificados foram posteriormente encapsulados em nanopartículas de quitosano (CS), que facilitam a entrada na célula, providenciando desta forma o suporte adequado para a entrega dos pre-miRNAs alvo no citoplasma das células neuronais. Após a síntese das nanopartículas, estas foram utilizadas para transfectar a linha celular N2a695 que sobreexpressa a BACE1 humana, permitindo a realização de estudos de avaliação da atividade dos pre-miRNAs. Neste contexto, o efeito isolado do pre-miR-9 e do pre-miR-29 nos níveis de

expressão de BACE1 e PSEN foi avaliado nesta linha celular. A análise dos níveis de RNAm por reação quantitativa em cadeia da Polimerase em tempo real (RT-qPCR) demonstrou uma diminuição da quantidade de RNAm de BACE1 e PSEN nas células transfectadas, não tendo os controlos apresentado diferenças significativas. O RNAm de BACE1 sofreu 42% de inibição pela ação do pre-miR-9 e 22% de inibição pela ação do pre-miR-29, comparativamente ao controlo de células não tranfectadas. No caso do RNAm de PSEN, este sofreu uma redução de 59% pela ação do pre-miR-9 e 14% pela ação do pre-miR-29, relativamente ao controlo de células não tratadas. Os resultados obtidos demonstram a ação inibitória do pre-miR-9 e pre-miR-29 no RNAm das proteínas BACE1 e PSEN, sugerindo uma potencial aplicação no tratamento da DA, com eventual efeito aditivo ou sinérgico dos pre-miRNAs estudados.

Palavras-chave

Doença de Alzheimer; Pre-miR-9 humano; Pre-mir-29 humano; Cromatografia de afinidade com arginina; Produção recombinante de pre-miRNA

Abstract

Alzheimer's disease (AD) is rising as a problem with epidemic proportions. In the latest years, promising genetic therapy technology has evolved with focus on microRNAs (miRNAs) as therapeutic agents since they can be used as translation repressors or messenger RNA (mRNA) degrading agents. This property can be exploited and applied to regulate the expression of some target proteins. AD and its possible treatment with miRNA technology is in the spotlight. Several studies in the literature have reported the link between two miRNAs, the miR-9 and the miR-29, and two important proteins, namely Beta-site amyloid precursor protein cleaving enzyme 1 (BACE1) and Presenilin (PSEN), which are part of the amyloidogenic pathway. Since the amyloid-β peptides (Aβ) start to excessively accumulate, due to the increased activity of the previously mentioned proteins, the amyloid plaque is formed. Actually, at the moment this is identified as one of the main causes of the disease. Recently, our group has studied the translation repression of human BACE1 by nanoparticle-mediated delivery of recombinant pre-miR-29 into neuronal cells. Therefore, the main goal of this project was also studying the effect of pre-miR-9 in BACE1 and PSEN expression levels and to assess the possible synergy between both of the nucleic acids.

Briefly, recombinant pre-miR-9 and pre-miR-29 were produced by *Escherichia coli (E. coli) DH5α*. Afterwards, the small RNA (sRNA) fraction was extracted by the guanidinium thiocyanate-phenol-chloroform RNA isolation protocol and purified by arginine affinity chromatography, using NaCl stepwise gradients. Both pre-miRNAs were purified by two distinct methods: a stepwise gradient with three steps and a stepwise gradient with two steps. Even though the stepwise gradient with three steps allowed the purification of both miRNAs, higher recovery was achieved when using the two stepwise gradients. The purified nucleic acids were then encapsulated into chitosan (CS) nanoparticles and used to transfect N2a695 cell lines. The efficacy of the translation inhibition of the BACE1 and PSEN mRNAs was assessed by quantitative real-time polymerase chain reaction (RT-qPCR) being demonstrated a decrease in BACE1 and PSEN mRNAs levels in the transfected cells whereas no significant difference in the control cells was observed. Mir-9 induced a greater BACE1 and PSEN mRNA inhibition than pre-miR-29, comparing to untreated control cells. In particular, BACE1 mRNA levels suffered a 42% of reduction after cells transfection with pre-miR-9 and 22% inhibition for pre-miR-29. For PSEN mRNA, it suffered 59% inhibition by pre-miR-9 and 14% inhibition by pre-miR-29. This study allowed the understanding of the effects of pre-miR-9 and pre-miR-29 on mRNAs and protein levels involved in the amyloidogenic pathway.

Keywords

Alzheimer’s disease; Human pre-miR-9; Human pre-miR-29; Arginine affinity chromatography; Pre-miRNA recombinant production

Table of Contents

List of Figures

List of Tables

List of Acronyms

3'UTR	3'-Untranslated Regions
A	Adenine
AD	Alzheimer's Disease
AGO	Argonaute
AICD	APP Intracellular Domain
APH-1	Anterior Pharynx-defective 1
APP	Amyloid Precursor Protein
ATP	Adenosine Triphosphate
ATPase	Adenosine Triphosphatase
Aβ	Amyloid-β
BACE1	β-site APP Cleaving Enzyme 1
BBB	Brain Blood Barrier
BCA	Bicinchoninic Acid
BERA	Bioengineered Non-coding RNA Agent
bp	Base pair
BSA	Bovine Serum Albumin
cDNA	Complementar DNA
CNS	Central Nervous System
CS	Chitosan
C_T	Threshold Cycle
DEPC	Diethylpyrocarbonate
DGCR8	DiGeorge Syndrome Critical Region Gene 8
DMEM	Dulbecco's Modified Eagle's Medium
DNA	Desoxyribonucleic Acid
dsRBD	Double-stranded RNA-binding Domain
dsRNA	Double-stranded RNA
DUF	Domain of Unknown Function
E. coli	*Escherichia coli*
EDTA	Ethylenediaminetetraacetic acid
EMEA	European Agency for the Evaluation of Medical Products
Exp-5	Exportin-5
FAD	Familial Alzheimer's Disease
FBS	Fetal Bovine Serum
FDA	Food and Drug Administration
FMRP	Fragile-X-mental-retardation Protein
GAPDH	Glyceraldehyde-3-phosphate Dehydrogenase
GTP	Guanosine Triphosphate
hnRNA	Heterogeneous Ribonucleoprotein
HPLC	High Performance Liquid Chromatography
LAL	Limulus Amebocyte Lysate
LB	Luria-Bertani
lpp	Lipoprotein
MID	Middle
miRNA	Micro RNA

mRNA	Messenger RNA
N	Amine groups
NCSTN	Nicastrin
OD	Optical Density
OnRS	Optimal non-coding RNA Scaffolding
P	Phosphate groups
PACT	Protein kinase R-activating Protein
PAZ	Piwi-Argonaute-Zwille
PCR	Poly Chain Reaction
pDNA	Plasmid DNA
PEI	Polyethylenimine
PEN-2	Presenilin Enhancer 2
PLGA	Poly(lactic-co-glycolic)
Poly-A	Poly-Adenylated
pre-miRNA	Precursor of miRNA
pri-miRN	Primary miRNA
PSEN1	Presenilin 1
PSEN2	Presenilin 2
RISC	RNA-Induced Silencing Complex
RNA	Ribonucleic Acid
RNA PolII	RNA Polymerase II
RNase	Ribonuclease
rRNA	Ribossomal RNA
RT-qPCR	Quantitative Real Time PCR
SAD	Sporadic Alzheimer's Disease
$sAPP_{\beta}$	Soluble APP_{β}
siRNA	Small Interfering RNA
snRNA	Small Non-coding RNA
sRNA	Small RNA
T	Thymine
TAE	Tris-acetic Acid
TBDMS	t-butyldimethylsilyl
TBE	Tris-Borate-EDTA
TOM	Tri-iso-propylsilyloxymethyl
TRBP	Tar RNA-binding Protein
tRNA	Transfer RNA
UTR	Untranslated Regions
WHO	World Health Organization

List of scientific communications

Poster communications related with this thesis

1. Joana Rodrigues, João A. Queiroz, Patrícia Pereira, Fani Sousa. Pre-miR-9 biosynthesis and purification: possible implications in Alzheimer's disease. I Congress in Health Sciences Research: Towards Innovation an Entrepreneurship - Trends in Endocrinology and Neurosciences. 26-28 november 2016, Covilhã, Portugal.
2. Joana Rodrigues, João A. Queiroz, Patrícia Pereira, Fani Sousa. Pre-miR-9 and pre-miR-29 biosynthesis and purification. XI Annual Cics-Ubi Symposium. 30 june-1july, 2016, Covilhã, Portugal.

Chapter I

Introduction

1.1. Biogenesis of microRNA

MicroRNAs (miRNAs) are small non-coding Ribonucleic Acid (RNA) molecules with approximately 22 nucleotides in length that contribute to the post-transcriptional regulation of gene expression [1–4]. The discovery of miRNA dates back to 1993, when Ambros and colleagues revealed that a small non-coding RNA (snRNA), lineage-4 (lin-4), regulated the larval development of the *Caenorhabditis elegans* [5]. MiRNA genes are very represented in the human genome and it is estimated that approximately 1 to 3% of the human genome encodes this form of RNA [1, 6–8]. MiRNA genes are distributed along intronic and exonic regions [6, 8–11] and according to Rodriguez and coworkers approximately 40% of all miRNAs are located within introns of protein-coding genes [12]. In these cases, regulatory factors and promoters can be shared between miRNA genes and their host genes [1], but there are cases in which even when in intronic coding regions, miRNAs may be transcribed independently from the rest [8, 9]. Thus, miRNAs genes can be expressed individually or in clusters [9–11, 13]. The miRNAs biogenesis process starts in the cell nucleus [6, 9, 11, 14]. Firstly, most miRNA genes are transcribed by RNA polymerase II (RNA PolII) giving rise to long primary transcripts of various lengths (usually 1–4 kilobases), called primary-miRNAs (pri-miRNAs) [1, 15–17]. This assumption comes from the fact that most pri-miRNAs have features of RNA PolII processing, namely 7-methyl guanosine-capped at the 5´ end and the poly-adenylated tail at the 3′ end [15, 17]. RNA PolII promoters are highly regulated explaining why different miRNA have so distinct expression levels [8]. The miRNAs can follow two distinct maturation pathways, the canonical or non-canonical biogenesis pathway. In particular, the canonical miRNA biogenesis pathway is depicted in Figure 1.

If the canonical pathway is considered, then the pri-miRNAs are processed by the microprocessor complex [13], which includes both the Drosha enzyme and the DiGeorge syndrome critical region gene 8 (DGCR8) [9, 18]. The DGCR8 is a double-stranded RNA binding protein [9] that recognizes the stem-loop and the flanking region of the pri-miRNA, helping Drosha binding to the correct site of the pri-miRNA [19]. Drosha is a ribonuclease (RNase) III [18, 20] that recognizes structures with large terminal loops of more than 10 nucleotides [2] followed by two helical turns with approximately 22 nucleotides of double-stranded RNA [7] linked to single-stranded RNA [2]. Consequently, Drosha cleaves approximately 11 nucleotides from the base of the hairpin embedded within the pri-miRNA [19] (Figure 1). Also, the activity of microprocessor complex is aided by different cofactors such as the RNA helicases p68 (DDX5) and the p72 (DDX17) and the heterogeneous ribonucleoproteins (hnRNPs) [2, 9]. The

resulting product of the RNase III-mediated cleavage is a long precursor of miRNA (pre-miRNA), with a hairpin structure of approximately 60 to 100 nucleotides that possesses two nucleotides overhang at the 3' end and a 5' phosphate (Figure 1) [7, 8, 21].

In the nucleus, Exportin-5 (Exp-5) associated with Ran Guanosine Triphosphate (GTP)-binding protein forms a nuclear transport receptor complex that allows the pre-miRNA transport from the nucleus to the cytoplasm (Figure 1) [3, 7, 9, 18, 22–24]. It has been shown that the complex Exp-5/Ran GTP recognizes a 2-3 base pair overhang of the pre-miRNA stem-loop structure [22, 25, 26]. Once in the cytoplasm, the pre-miRNA binds to Dicer protein. The cytoplasmic Dicer protein is a RNase III-type enzyme [8] that contains functional domains: two RNase III domains (forming one catalytic center) [8, 9] and two double-stranded RNA binding domains (DUF and dsRBD) [9]. In addition to these domains, Dicer also contains helicase Adenine Triphosphatase (ATPase)/RNA and PAZ (Piwi-Argonaute-Zwille) domain [8, 9] and its cofactors Tar RNA-binding protein (TRBP) [18, 27] and Protein Kinase R-activating protein (PACT) [27, 28]. Current research suggests that the PAZ domain is capable of binding 2 nucleotides 3' overhang of single-stranded RNA and, therefore, it may recognize the products resulting from Drosha activity [29]. Thus, after the recognition by Dicer of the 2 nucleotides 3' overhang of pre-miRNA to the exact cutting site (approximately 20 nucleotides away) [30], each RNase III domain cuts one RNA strand, removing the terminal loop of the pre-miRNA [9, 20]. The resulting product is a double-stranded miRNA (miRNA-miRNA* duplexes) with approximately 22 nucleotides with two 2 nucleotide 3' overhangs (Figure 1) [2, 13].

Afterwards, the double-stranded miRNA is loaded into a multisubunit complex termed RNA-induced silencing complex (RISC) [1, 9]. This complex is composed by Argonaute (AGO) proteins [9, 13, 18] which have endonuclease activity [11], TRBP and also other components: RNA-binding protein fragile-X-mental-retardation protein (FMRP) [31], p-body marker GW182 [32] and decapping activator RCK/P54 [33]. AGO are strongly basic proteins [20] that contain an amino-terminal domain [2], a PAZ domain (binds the 3' end) and middle (MID) domain (binds the 5' monophosphate) [2, 34]. During loading to RISC, one of the two strands of the duplex RNA (miRNA-miRNA*) is released and degraded, called passenger strand (also referred to as miRNA*), whereas the other strand is incorporated into RISC, called guide strand (also referred to as miRNA) (Figure 1). This selection is determined by the relative thermodynamically stability of the two ends of miRNA duplexes, thus, the strand less stable at the 5' end (weaker hydrogen bonds) is loaded into RISC [8, 9, 13, 18].

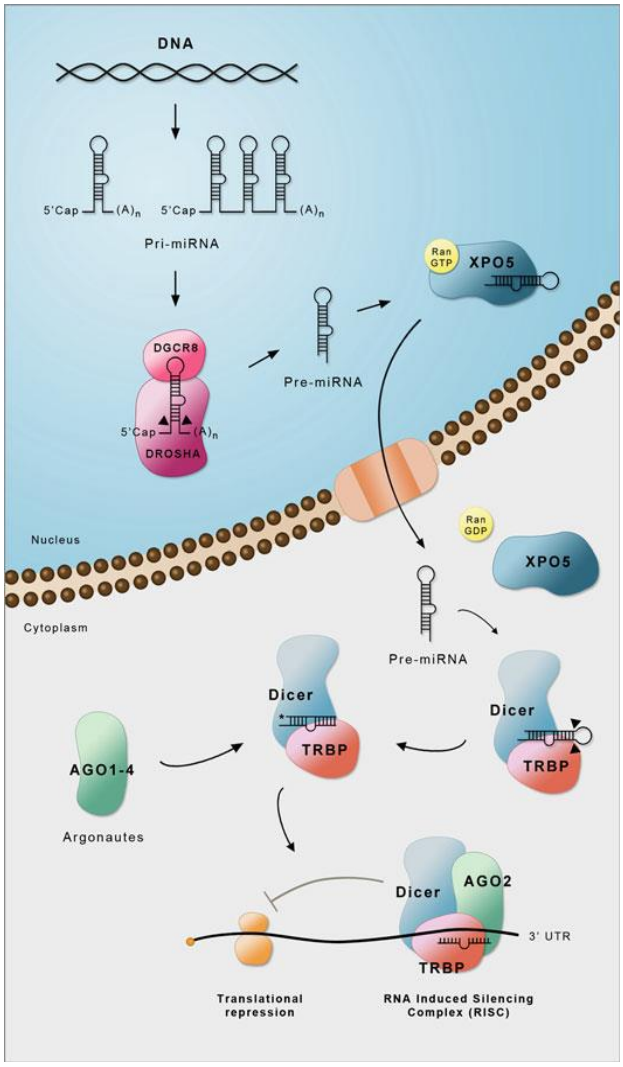

Figure 1 - Biogenesis of miRNAs. This process starts by pri-miRNA transcription by RNA PolII, then it is processed into pre-miRNA by the microprocessor complex in the nucleus. Afterwards, the pre-miRNA is transported by Exp-5/Ran-GTP to the cytoplasm, where it is processed by Dicer complex and finally the mature miRNA strand is chosen by the RISC complex [9].

Alternatively, if miRNAs follow the non-canonical biosynthesis pathway they do not undergo any processing by Drosha nor Dicer. Instead, pre-miRNAs are generated by splicing in the nucleus and are transferred into the cytoplasm, like in the canonical pathway, with the help of Exp-5. Then, AGO proteins binding occurs without Dicer intervening [2].

1.2. MicroRNA functions

In the past two decades, miRNAs have been extensively studied due to the discovery of RNA interference (RNAi) functions. MicroRNAs are involved in many cellular events and can act as regulators of metabolism, cell cycle, stress response, stem cell self-renewal, determination of the cell fate, viability, differentiation, adhesion, proliferation, developmental timing, genome integrity and stability, heterochromatin formation and maintenance of cellular integrity [1, 6, 9–11, 18, 35]. Consequently, they control organogenesis [6] and induce, according to the levels of their expression, embryogenesis, neurogenesis, adipogenesis,

osteogenesis and myogenesis [13, 19, 36]. More specifically, miRNAs are also reported to be responsible for immune response, insulin secretion, neurotransmitter synthesis, circadian rhythm, cellular migration, epithelial to mesenchymal transition and control of estrogen receptors [9, 10]. However, one of the most important and studied specific functions of the miRNAs is their capacity to regulate gene expression by post-transcriptional control of the messenger RNA (mRNA), through translational repression or degradation. On the other hand, they may also exert the opposite function by enhancing gene expression [10, 37]. Thus, miRNAs have the ability of interacting with specific mRNAs and, without changing their levels, controlling protein levels [20].

As mentioned above, after the selection of the guide strand of microRNA, it is loaded onto the RISC that identifies the target mRNA, based on sequence complementarity with the miRNA (Figure 1) [6, 11]. This interaction occurs between specific sequences (called 'seed' sequence composed by 2-8 nucleotides) located in 5' end of the miRNA and the 3' untranslated region (3'UTR) of their target mRNA [6, 9–11, 18, 38]. The regulation of gene expression mediated by miRNA depends on the degree of complementarity between miRNA-mRNA and of the AGO that is recruited to the complex, conducting to two possible types of responses, namely mRNA translation repression or endonucleolytic cleavage of the mRNA (Figure 1) [1, 9, 11]. In mammals, there are four AGO proteins (AGO 1-4). The AGO 1, AGO 3 and AGO 4 have translation repression activity, whereas AGO 2 possesses slicer activity, resulting in the cleavage of the complementary sequence of the target mRNA. For the mRNA translation repression only few complementary bases are necessary [9, 11]. If the AGO 2 protein is the one connected to the RISC, a perfect complementarity is needed so that cleavage and degradation of the target mRNA may occur [11]. Higher specificity can also be achieved if there is pairing between nucleotides that are not part of the 'seed' region [1, 38]. MiRNAs may target more than one mRNA sequentially once they are not altered or degraded after the events [1] and actually one miRNA may target many different mRNAs while a particular mRNA may also be targeted by diverse miRNAs [39].

Of course the possible pharmacological applications of miRNAs cannot be left behind since there is a demand for better treatments with less side-effects [36] and, as a consequence, the investigation on miRNA-based therapies has been evolving in areas like cancer, neurodegenerative diseases, psychiatric, cardiovascular diseases, metabolic diseases, viral infections, hypertension and stroke and immune dysfunction [13, 18]. Several online platforms, namely 'PhenomiR' (http://mips.helmholtz-muenchen.de/phenomir/, website accesses on September 1st), 'OncomiRDB' (http://tools4mirs.org/software/mirna_databases/oncomirdb/, website accesses on September 1st) and 'microRNA Disease Database (HMDD)' (http://210.73.221.6/hmdd, website accesses on September 1st), include detailed information about the correlation between miRNAs and several diseases.

1.3. Alzheimer's Disease ("amyloidogenic pathway")

Alzheimer's disease (AD) was first described by Alois Alzheimer in 1907 on his publication and, currently, it is the main cause of dementia in the world, particularly in elderly [40–43]. For example, it is estimated that AD will affect more than 16 million people in America by 2050, constituting a growing health problem for our societies due to the increased life expectancy, and the lack of progress in identifying effective diagnosis and treatment modalities [44, 45]. AD can be classified in Sporadic Alzheimer's disease (SAD) or Familial Alzheimer's disease (FAD) [46]. The two types of Alzheimer can be diagnosed in early-onset (refers to people with less than 65 years old) and in late-onset (refers to people older than 65 years old) [41, 46]. The SAD type reports most AD cases and can be caused by diverse factors such as genetic and environmental [46]. Otherwise, FAD is diagnosed when there are more than one individual with the disease in the same family in more than one generation and it exists mainly because of autosomal dominant mutations in three genes, namely in the Amyloid precursor protein (APP), Presenilin 1 (PSEN1) and/or Presenilin 2 (PSEN2) [21, 46]. AD has adverse consequences like cognitive and synaptic dysfunction, behavioral impairment and neuronal death [42, 44, 47]. Moreover, the areas of the brain that are mainly affected are the hippocampus, the association cortices and subcortical structures [48].

One molecular mechanism that has been implicated in the AD pathology is the formation and accumulation in the brain of toxic Amyloid-β (Aβ) peptides that form amyloid plaques (also known senile plaque) [40, 42, 45, 47, 49]. These peptides, when present in low concentrations, act as neurotrophic and signaling molecules [50]. On the other hand, Aβ peptides can accumulate and agglomerate as dimers and higher oligomers in the extracellular space causing microgliosis, astrocytosis and neuritic dystrophy [47, 51, 52]. These Aβ peptides result from the sequential proteolytic cleavage of the APP [42] which is an integral membrane protein [53, 54] with an extracellular domain (sAPP) [50], a single membrane-spanning domain and a cytosolic domain [50, 53], as shown in Figure 2. It has been shown that APP may adhere to extracellular molecules or other cells and also owns important roles in brain development and protection [50, 51], being involved in cholesterol and calcium metabolism, synaptogenesis, transmembrane signal transduction, axonal transport and gene transcription [51].

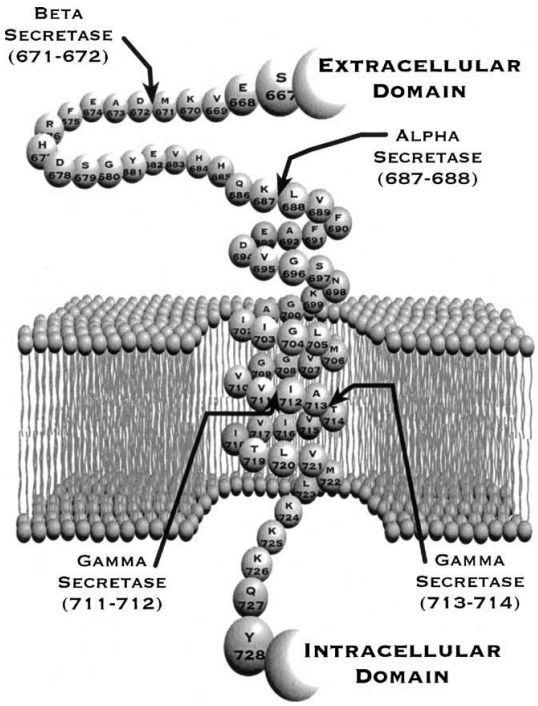

Figure 2 - APP representative structure. The arrows indicate the sites where different secretases can act to induce APP cleavage [51].

APP may be cleaved by the action of α-secretase followed by the action of γ-secretase ("non-amyloidogenic pathway") or, alternatively, APP may be cleaved by β-secretase followed by the cleavage with γ-secretase (“amyloidogenic pathway”) (Figure 3) [44, 53], originating the Aβ peptides. In detail, in the “amyloidogenic pathway”, APP is initially cleaved by the β-secretase (also known as β-site APP-cleaving enzyme (BACE)), a site-specific aspartic-acid protease found in neuronal cells [42, 51, 53, 55] that cleaves exactly between specific amino acids of APP (cleavage between residues 671 and 672 of APP [40, 51] or between residues 596 and 597 of APP_{695} [51]). The action of this enzyme results in the detachment of the soluble APP_{β} ectodomain ($sAPP_{\beta}$) from the remaining peptide of 99 amino acid long (C99) still connected to the membrane (Figure 3) [42, 49, 53, 55–57].

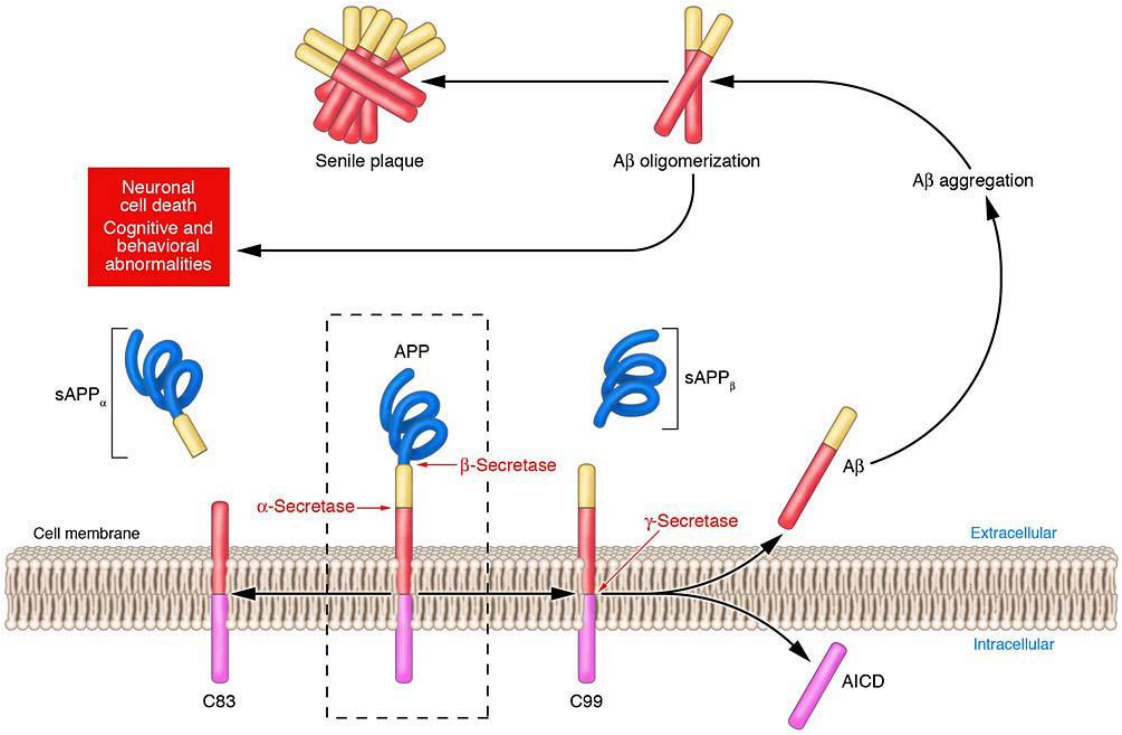

Figure 3 - The non-amyloidogenic and amyloidogenic pathways of APP processing [58].

The resulting fragment of APP (C99) is then cleaved by the γ-secretase complex. γ-secretase is a membrane complex composed by Presenilin (PSEN), Nicastrin (NCSTN), Anterior Pharynx-defective 1 (APH-1) and Presenilin enhancer 2 (PEN-2) [59-61]. Presenilins are transmembrane proteins with cytoplasmic N-termini and C-termini and eight transmembrane domains [40]. The action of γ-secretase gives rise to an intracellular domain of APP of approximately 50 amino acids (AICD) [60] and a variety of Aβ peptides with heterogeneous carboxyl-terminus ranging from 38 to 43 amino acids (Figure 3) [55]. This reaction is not site-specific once it may mostly origin $A\beta_{40}$ peptides (if the cleavage takes place between residues 712-713 [40]) and $A\beta_{42}$ peptides (if the cleavage takes place after residue 714 [40]). $A\beta_{40}$ peptide is the most predominant form contributing for more than 90% of total Aβ, whereas $A\beta_{42}$ is more toxic because of its low solubility in aqueous media [53].

Several research groups have demonstrated that the overexpression or high activity of BACE1 and γ-secretase may positively influence AD development, suggesting that BACE1 and γ-secretase deregulation is directly implicated in AD pathogenesis through the formation of toxic Aβ peptides [62, 63]. Thus, it has been established that reducing BACE1 and γ-secretase expressions may delay or even reduce AD progression. Actually, it was already described the deregulation of some miRNAs levels in patients with AD, namely the miR-9 and the miR-29 [45]. In addition, these miRNAs have been described to target the UTR of BACE1 and PSEN mRNAs, also altered in pathological conditions as depicted in Figure 4 [45, 64, 65].

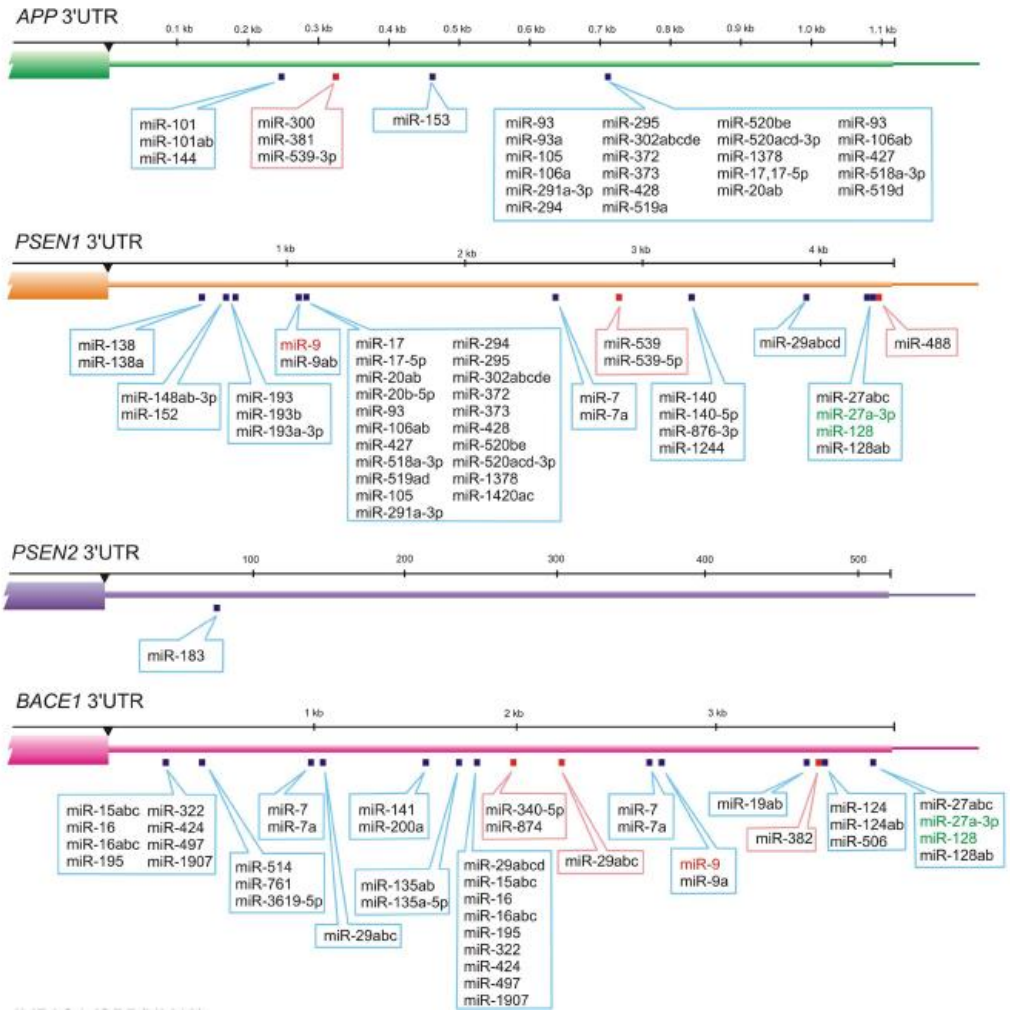

Figure 4 - MicroRNAs and their evolutionary-conserved sites in 3' UTR-gene regions for AD genes. Red boxes contain miRNAs that are conserved among mammals and blue boxes contain miRNAs conserved among vertebrates. MiRNA-9 that is up-regulated in AD neocortex, hippocampus, and in age-related macular degeneration affected retina is indicated in red. MiRNAs that are most abundant in control temporal lobe association neocortex are indicated in green. Adapted from Lukiw and coworkers [66].

1.4. miR-9 and miR-29: The role in the "amyloidogenic pathway"

The expression levels of miR-9 and miR-29 family seems to be altered in brains of AD patients and they have both been associated with different molecular pathways involved in the pathogenesis of AD [61, 64, 67]. MiR-9 is the most abundant miRNA in the human brain [61] and it is encoded by three genes miR-9-1, miR-9-2 and miR-9-3 [68]. Mature miR-9 is composed of approximately 23 nucleotides (www.mirbase.org, website accessed on september 1st). The miR-29 family (miRNAs that share the same "seed" sequence [62]) comprises miR-29a, miR-29b-1, miR-29b-2 and miR-29c [62, 69]. Mature miR-29 has approximately 22 nucleotides (www.mirbase.org, website accessed on september 1st). These two miRNAs have been shown to be downregulated in brains affected by AD [21, 64, 67, 70].

MiR-29 has an important role in the β-amyloid pathway as it targets the BACE1 mRNA [48, 62, 67, 71] and so it has been proposed for miR-9 [48, 67, 72]. On the other hand, miR-9 was also predicted to target the 3'-UTR of PSEN1 [48, 64, 67] and low levels of this miRNA were already found in the cerebellum, hippocampus and media frontal regions of patients with AD [69]. PSEN1 is a protein integrant of the catalytic core of γ-secretase [46]. Hébert and co-workers demonstrated that the loss of the cluster miR-29a/b-1 leads to an increase in the expression of the BACE1 protein levels in patients with SAD and that the introduction of synthetic miR-29 reduces secretion of Aβ peptides [64]. Another study correlated the density of amyloid plaques and miR-9 levels, from which was concluded that a decrease in miR-9 levels was related to amyloid plaque increase [72] and this situation was also demonstrated for miR-29 where low levels of miR-29 were associated with an increase in Aβ peptides and BACE1 concentrations [67, 69]. Furthermore, it was also demonstrated that mice overexpressing miR-29c presented downregulated BACE1 and this result was also demonstrated *in vitro* [71]. These findings raised the opportunity to use miR-29 and miR-9 as therapeutic products to silence BACE1 and PSEN1 protein expression, based on the hypothesis that reducing the level of these proteins is a protective strategy for AD.

The investigation in this field is growing since it presents amazing perspectives and it also brings benefits as the specificity, efficiency and long-lasting (days/weeks) of the treatment avoiding high dosage administration [18]. In this context, nucleic-acid therapeutics arose as a promising alternative to small-molecule drugs and protein therapeutics [36, 73], when neurodegenerative diseases are focused and a deregulation of miRNAs is considered the main cause [74]. A very important fact to consider when studying new drugs is the delivery system. In the case of neurodegenerative diseases, most of the treatments are directed to the central nervous system (CNS), which possess selective barriers, among which stands out the brain blood barrier (BBB). The BBB is very selective, preventing the passage of a wide number of molecules [75]. Due to this, the vectors for non-coding RNA delivery are important factors [73, 76] as, for example in the case of miR-9 or miR-29 delivery to the brain, it is required a technology that goes through the BBB. In the past few years, the nanoparticle-based delivery systems have evolved, leading to different suitable nanoparticle carriers that go through the BBB, among which chitosan is mentioned [75, 77], being a biodegradable, biocompatible, biodegradable and presenting low toxicity material, which is required [78]. In a recent study, Pereira and coworkers analyzed different materials as polyplexes carrying small RNA (sRNA) and concluded that the chitosan (CS) is a very suitable option as nanocarrier [79]. For these reasons and supported by the investigation described in the previous sections, miR-9 and miR-29 may be considered as important molecules to be studied as therapeutics in AD.

1.5. Recombinant production of miR-9 and miR-29

In order to obtain the functional miRNA for pharmacological applications, it is still necessary to improve the production process, to achieve higher product titers (milligram quantities)

while maintaining maximal product quality, stability, safety and biological activity. Currently, there are three different ways for RNA manufacturing, namely the chemical synthesis (via phosphoramidite chemistry) [36, 80, 81], enzymatic methods (*in vitro* transcription) [36, 80] and recombinant production (also known as *in vivo* production) [36, 80, 82]. *In vivo* production of RNA molecules is considered the most reliable option, as it is expected to be a more economical, feasible and accurate method [80].

Chemical synthesis allows the introduction of molecular modifications in the synthetic RNA molecules, for example through the addition of t-butyldimethylsilyl (TBDMS) or tri-iso-propylsilyloxymethyl (TOM) in RNAs to protect their 2'-hydroxy groups. These groups that are added to the RNA may be removed with fluoride and purified by high performance liquid chromatography (HPLC) [36, 81]. Apart from these modifications for RNA protection, other changes (mostly desired on the sugar or phosphate backbone) can be made with different purposes, namely to promote resistance to nucleolytic degradation, to increase RNA half-life, to hinder renal clearance by favoring the binding to plasma proteins, or to increase metabolic stability. Although the chemical synthesis process allows the selection of the sequence to be modified, there are some negative points such as the low yield, high costs of the process that are proportional to the length of the oligonucleotide being synthesized and the uncertainty that the modified RNA will remain stable and maintain its biological activity [36].

The *in vitro* transcription is a simple approach used to obtain single-stranded RNA molecules for different applications including *in vitro* translation, detection assays and structural and functional studies. As the name indicates, this process is based in the transcription of a linearized DNA template, PCR products or synthetic oligonucleotides to specifically generate RNA sequences with variable lengths, by the action of RNA polymerase. The promoter of the sequence is very important because the success of the entire course relies on it. For example T7 promoter can be used with T7 RNA polymerase [36, 80]. For this reason, this approach is generally less efficient because it is necessary to transcribe the DNA to RNA and it is dependent of the action of the RNA polymerase. In addition, the transcripts must be posteriorly purified to remove the contaminants derived from the transcription reactions. Although this approach has been well established for the production of RNAs, serious problems have been described such as the lack of reliability of the T7 RNA polymerase when transcript length increases and certain RNA products display heterogeneity at 3' and 5' ends [36, 82]. A new approach that intends to overcome this problem is the conjugation of *in vitro* transcription followed by Dicer processing to obtain the mature and functional RNA molecule [36].

In vivo expression of recombinant RNA molecules is a fermentation-based method using prokaryotic hosts (usually *E. coli* strains) to obtain RNA molecules that already possess the posttranscriptional modifications that favor their stability and correct folding (as schematized in Figure 5). It is important to emphasize that the biosynthesis of these molecules can be

greatly improved and optimized for example at the promoter level. Thus, different promoters may be chosen, such as natural *E. coli* promoter (endogenous RNA), inducible *lac* promoter (and derivatives), lipoprotein (*lpp)* gene promoter, the T7 transcription system, or the *rrn* promoter [82]

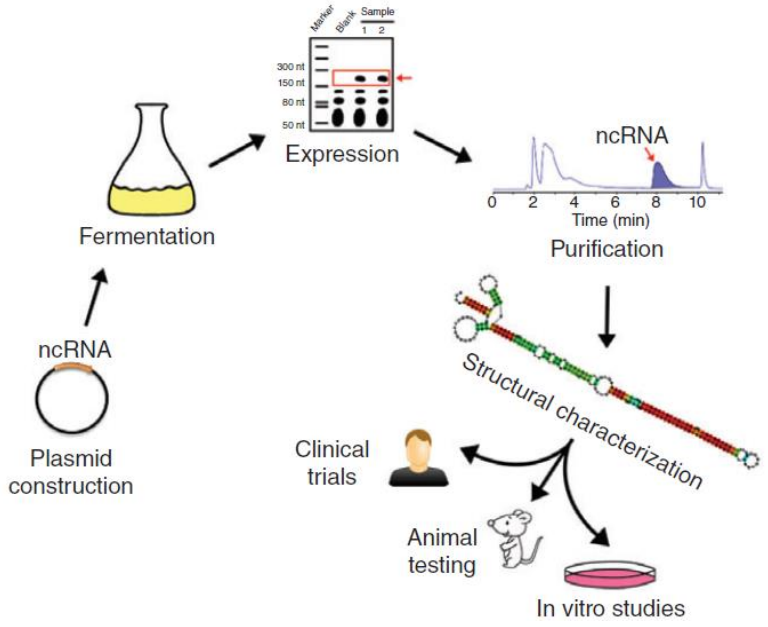

Figure 5 - Recombinant production of ncRNA and further investigation [36].

RNA molecules are highly fragile, sensitive and susceptible to RNases activity within the fermentation medium or even out of it and to overcome this situation several strategies have been developed such as the use of bioengineered non-coding RNA agents (BERAs) like transfer/ribosomal/optimal non-coding RNA scaffolds (Figure 6) [36, 82].

Scaffolds were also explored at different levels and their choice relies on natural properties of specific types of RNA. Transfer RNAs (tRNAs) are highly resistant to heat-denaturation and are able to escape nucleolytic cleavage due to its complex structure (stable three-dimensional four-leaf clover structure) [36, 82]. Thus, in 2007, it was reported the use of tRNA as a scaffold for *in vivo* production of large quantities of recombinant RNA molecules [83]. The tRNA-based recombinant RNA approach is based on the substitution of the anticodon region by the interest RNA (including RNA aptamers, hammerhead riboswitch RNAs and pre-miRNAs, among others) [36, 82], while the acceptor TψC and D stems stay to maintain the tertiary structure of tRNA [36, 84] so that the host cells would process the recombinant RNA as tRNA species [36]. The final products may be obtained by subjecting the complex structure to the action of RNases [36, 80] or ribozymes [36].

In the case of ribosomal RNA (rRNA) scaffolds (e.g. 16S small ribosomal subunit and the 5S and 23S), it may be stated that these structures are very stable and easily and widely expressed within *E. coli*. Again, the interest sequence of recombinant non-coding RNA is included into

stem II and replaced the stem III loop B and C regions of the 5S rRNA [36, 82]. This manipulated sequence can be transcribed using rRNA gene promoters rrnB P1 and P2 promoters, and the transcription is terminated by rrnB T1 and T2 terminators, followed by product purification. The yield of this process rounds the 90% [36].

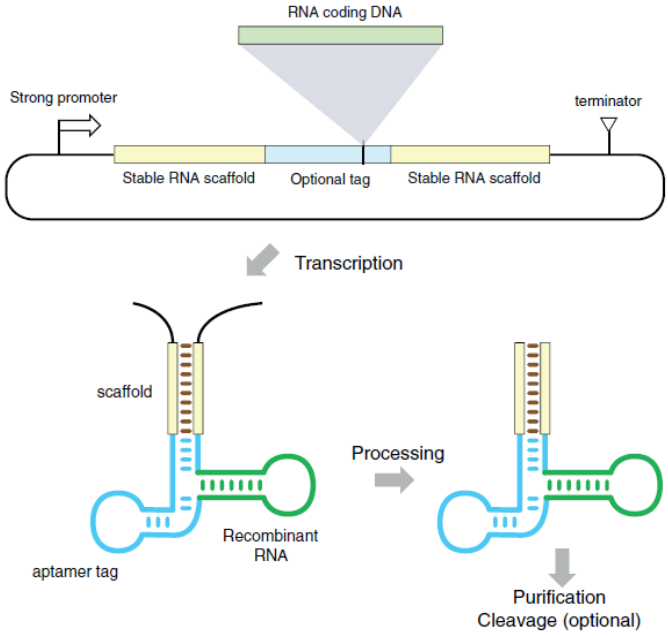

Figure 6 - Recombinant RNA expression scheme. Exemplified recombinant RNA (green portion) within scaffolds (brown portion) and RNA tags (blue portion) [82].

Another branch within this category is the optimal non-coding RNA scaffolding (OnRS) which is basically an RNA scaffold which gives high yields (milligrams of RNA per liter of bacterial culture) of interest RNA (such as miRNAs, small interfering RNAs (siRNAs) and RNA aptamers). For example, the combination of a tRNA scaffold with pre-miRNA genes increased substantially the *E. coli* production of the same pre-miRNA which was successfully processed within carcinoma cells to mature functional miRNA [85]. OnRS have the advantage of carrying small or large single-stranded RNA molecules and, of course, the exploration of the structure for sequences substitution for interest double-stranded RNA [36].

In general, the recombinant approaches are usually more cost-effective and simple than the chemical and enzymatic synthesis methods to produce large amounts and structurally stable miRNAs [82]. For all these reasons, the *in vivo* techniques are important references for the development of a sustainable and safe recombinant miR-9 and miR-29 production method, avoiding the employment of toxic and potentially RNA degrading purification methods that are commonly used to eliminate contaminants present in RNA mixtures obtained from chemical synthesis or *in vitro* transcription [80].

1.6. Affinity chromatography using amino acids for miRNA purification

In order to use miRNAs as therapeutic products it is also necessary to ensure its purity, integrity, stability, safety and biological activity. Thus, the development of efficient, reliable, fast and more robust procedures for RNA purification is crucial to guarantee their structural and functional stability as well as their biological activity.

Affinity chromatography is a type of liquid chromatography (Figure 7) that takes advantage of multiple non-covalent interactions, such as hydrogen bonds, cation-π interactions, electrostatic and hydrophobic interactions, van der Waals and dipole-dipole forces, that occur between the target biomolecule and the immobilized affinity ligand (biological agents as specific ligands) [18, 86–88]. The capacity to establish different types of interactions is a major advantage of this kind of chromatography, once it allows to achieve higher specificity, purity and recovery levels of the target RNA molecule [86, 88]. It is also a simple separation method because less elution steps are necessary for the whole process [86, 87]. The elution processes applied depend on the immobilized ligand, the physicochemical and thermodynamic nature of the molecular interactions involved and, of course, of the molecular/structural properties of the target RNA (size, charge, secondary structure, hydrophobicity). Thus, the elution of a target RNA can be achieved either by specific (using competitive ligands) or non-specific elution conditions (by changing the pH, ionic strength or polarity) [86]. Several affinity chromatographic strategies have already been developed in order to isolate or purify RNAs, for example oligo(dT) chromatography, RNA affinity tags and amino acid-based affinity chromatography [86].

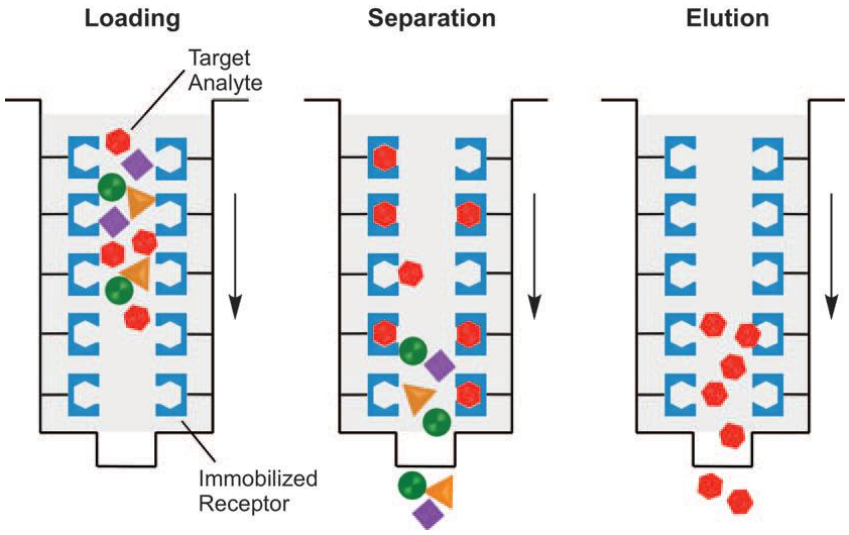

Figure 7 - The three major steps concerning affinity chromatography: sample loading, separation of different species present in the sample and elution [89].

Briefly, oligo(dT) chromatographic process is based on the specific affinity of base pairs (A-T), through hybridization of poly-A sequences inside the target RNA to anchored oligo-dT.

Although it presents most of the advantages of affinity chromatography described above, this technique does not allow the isolation of non-polyadenylated RNA [86].

The strategy of using RNA affinity tags allows the association of biotinylated synthetic miRNAs with streptavidin matrices or the immobilization of RNA aptamers with high affinity for streptavidin or streptomycin for the purification and selective recovery of the tagged RNAs. The recovery of bound RNA can be obtained through competitive elution strategies with biotin or dextran or through cleavage by a protease with a recognition site that is incorporated along with the affinity tag [18, 86]. Sometimes, along the process it is necessary to use denaturing conditions or it may be required the application of several sequential purification steps [86].

Regarding affinity chromatography using amino acids as affinity ligands (called amino acid-based affinity chromatography), it can be stated that it is an effective technique for isolation and purification of different RNA species that exploits specific interactions occurring between the amino acids and nucleic acids. The RNA intended for pharmaceutical purposes should be pure, free from contaminants (such as genomic DNA (gDNA), proteins, endotoxins or organic solvents) and must be in its native conformation, preserving their biological activity [86, 90]. Some amino acids and amino acid derivatives such as Arginine [86, 91], Histidine [86, 92], Lysine [93], *O-Phospho*-L-Tyrosine [87] and Agmatine [90] have already been tested as potential affinity chromatographic ligands for the purification of diverse RNA molecules. The arginine-affinity chromatography is a very promising field in chromatography because it mimics the natural and very dominant interactions occurring at biological level between proteins and RNA [86]. Moreover, positively charged amino acids like arginine are good alternatives to efficiently purify and isolate all functional classes of RNA (small RNA, rRNA, tRNA and pre-miRNA) from other isoforms and host impurities since their groups interact with the exposed negative charges of the RNA phosphates, allowing the required selectivity [18, 90, 94]. In a practical point-of-view, the application of arginine as specific ligand has advantages over other strategies because RNA retention is established with lower salt concentration and species are eluted with a slight increase in ionic strength. These stronger and more selective interactions maybe due to the arginine side chain that allows several contact points between arginine and the RNA backbone or bases (in particular guanines) [18, 86, 88].

In the last years, monolithic supports have emerged as alternative chromatographic supports, presenting several advantages such as, high external porosity, high sample distribution, excellent mass transfer properties, a huge quantity of accessible binding sites (high binding capacity), reproducible separation and the possibility to use higher or lower flow-rates at large or small scales [18, 90]. A very important factor is the fragile nature of RNA and in this matter monoliths provide a much faster elution so that the RNA is less affected by the retention conditions which could degrade it and consequently lead to activity loss [18].

In our research group different amino acid ligands have already been studied for the purification of nucleic acids. Martins and co-workers reported the isolation of sRNA and ribosomal RNA (rRNA) from lysate samples by employing affinity chromatography using histidine ligands [92]. Different approaches were also previously described for the purification of pre-miR-29, namely by using O-*phospho*-L-tyrosine affinity chromatography [87], arginine affinity chromatography [91], lysine affinity chromatography [93] and agmatine affinity chromatography with monolithic support [90]. In the case of arginine affinity chromatography, NaCl stepwise gradients were used allowing pre-miR-29 purification in one single step and with high recovery rate [91]. In addition, the purification using lysine affinity chromatography allowed the isolation of pre-miR-29 using $(NH_4)_2SO_4$ stepwise gradients with a good recovery rate [93]. In a similar way, the pre-miR-29 profile purified with O-*phospho*-L-tyrosine and $(NH_4)_2SO_4$ stepwise gradients also resulted in a satisfactory RNA recovery [87]. Agmatine monolith was a suitable and versatile chromatographic support for pre-miR-29 isolation, since it allowed the RNA recovery with different methods, such as using a $(NH_4)_2SO_4$ stepwise gradient, a NaCl stepwise gradient and applying competition assays with arginine in the mobile phase [90].

Several techniques have already been exploited in order to isolate different sRNA from RNA lysates. It is important to focus that there is the need to achieve sRNA isolation by using chromatographic techniques that are simpler, more efficient and robust. In the present work pre-miR-29 and pre-miR-9 were purified by arginine affinity chromatography with a monolithic support, exploiting different approaches.

Chapter II

Materials and Methods

2.1. Materials

The plasmid pBHSR1-RM (kindly provided by Dr. Yo Kikuchi) was used as the expression vector. Restriction enzymes including Stu*I* and Xba*I* were purchased from Takara (Shiga, Japan) and New England BioLabs (Ipswich, MA), respectively. T4 DNA ligase was used as recommended by the manufactures (Promega, Madison, USA). Supreme NZYTaq 2x Green Master Mix was purchased from NZYTech (Lisbon, Portugal). Primers were synthesized by StabVida (Caparica, Portugal). "PCR clean-up, gel extraction" kit was from Macherey-Nagel (Duren, Germany). Hyper Ladder I (Bioline, London, UK) was used as DNA molecular weight marker. The sequences of pre-miRNAs were obtained from the miRBase (http://www.mirbase.org/index.shtml). For *E. coli DH5a* culture, it was used tryptone and yeast extract from Bioakar (Beauvais, France), glycerol from Himedia, sodium chloride and K_2HPO_4 from Panreac (Barcelona, Spain), KH_2PO4 from Sigma-Aldrich (St Louis, MO, USA), kanamycin from Thermo Fisher Scientific Inc. (Waltham, USA) and agar was from Pronalab (Mérida, Yucatán). GreenSafe Premium and Miniprep kit were purchased from NZYTech (Lisbon, Portugal). Guanidine thiocyanate salt, isoamyl alcohol and sodium citrate were from Sigma-Aldrich (St Louis, MO, USA), N-laurosylsarcosine from Fluka Analytical (United Kingdom) and isopropanol from Thermo Fisher Scientific Inc. (Waltham,USA). β-Mercaptoethanol, sodium acetate anhydrous and chloroform were from Merck (Whitehouse Station, USA) and glaciar acetic acid was purchased from Chem-Lab (Zedelgem, Belgium). All chromatographic buffers were freshly prepared using 0.05 % Diethylpyrocarbonate (DEPC, Acros Organics, New Jersey, USA) treated water and where filtered through a 0.20 µm pore size membrane (Schleicher Schuell, Dassel, Germany). All the materials used in the experiments were RNase-free. The Maxima® SYBR Green/Fluorescein qPCR Master Mix (Thermo Fisher Scientific Inc.) was used for gDNA quantification.

2.2. Methods

2.2.1. Polymerase Chain Reaction (PCR)

The plasmid pBHSR1-RM encoding the pre-miR-29 sequence (pBHSR1-RM-pre-miR-29b) [80] was used as template in a Polymerase Chain Reaction (PCR). Specific primers (Forward – 5'-CGAGGCCTGGGGTTGGTTGTTATCTTTGGTTATCTAGCTGTATGAGTGGTGTGGAGTCTTCATAAAGC TAGATAACCGAAAGTAAAAATAACCCCAATCATACCGCTGTCAGCCGTGCAAG-3' and Reverse – 5'-CATCTAGAGCTCATGCCCTTGAGATCGGCC-3') were used to amplify the DNA fragment containing the encoded sequence of pre-miR-9. In each tube, a mix was prepared containing

0.125U Supreme DNA polymerase, 50 mM magnesium chloride, 150 nM of each primer and nuclease free water up to a final volume of 25µL.The PCR was optimized for these primers and the program was: 5 minutes at 95 ºC for denaturation, 40 cycles with three different steps – 95ºC for 30 seconds, 60ºC for 30 seconds and 72ºC for 15 seconds–and5 minutes at 72 ºC for final extension. The PCR products were purified according to "PCR clean-up, gel extraction" kit instructions and analyzed by 1% agarose gel electrophoresis, in order to confirm the presence and purity of amplicons.

2.2.2. Enzymatic digestions with Stu*I* and Xba*I*

The pBHSR1-RM-pre-miR-29b plasmid and PCR products of pre-miR-9 were digested with Stu*I* and Xba*I* restriction enzymes. 1 µg of pre-miR-9 sequence and 1 µg of the pre-miR-29 containing vector were separately digested with Stu*I* according to the manufacturer's instructions (''StuI Takara Biotechnology'') in a 20 µL reaction at 37 ºC for 2 hours. Afterwards, products were purified according to ''PCR clean-up, gel extraction'' kit instructions. Then, the digestions with Xba*I* were carried out according to manufacturer's instructions (''XbaI New England BioLabs'') in a 20 µL reaction at 37 ºC for 2 hours. Products were also purified according to ''PCR clean-up, gel extraction'' instructions. Digestions were confirmed by 1 % agarose gel electrophoresis. A 1 % agarose gel electrophoresis was performed with the digested vector to separate it from the pre-miR-29 sequence. After this, the band of the gel containing the vector was extracted with a bistoury and the sequence was separated from the agarose gel according to ''PCR clean-up, gel extraction'' kit instructions (Duren, Germany). The concentration of the fragment and of the vector was determined by NanoPhotometer (IMPLEN, United Kingdom). The cloning process was carried out according to ''Promega t4 DNA Ligase'' instructions (Madison, USA). The insert:vector ratio chosen to obtain the final vector was 3:1. In the reactional tube, 100 ng of digested vector, 40 ng of pre-miR-9 insert and approximately 1 U of T4 DNA Ligase were added. The reaction mixture was incubated for 16 hours at 4 ºC.

2.2.3. Agarose Gel Electrophoresis

This technique was performed to analyze the purity and stability of the PCR products and samples obtained from RNA extraction. The samples were prepared with loading buffer (bromophenol blue, glicerol and Tris Buffer) and injected into a 15-cm-long 1 % GSR agarose LE gel (Grisp, Porto, Portugal) stained with 0.01 % GreenSafe Premium. Electrophoresis was carried out in 1X Tris-acetic acid (TAE) buffer (40 mM Tris-base, 20 mM acetic acid and 1 mM Ethylenediaminetetraacetic acid (EDTA), pH 8.0) and run at 130 V for 30 minutes. The gels were revealed under UV light in an UVITEC Cambridge Fire-reader XS D-56-26LM system (Cambridge, UK).

2.2.4. Preparation and transformation of competent *E. coli DH5a* cells

For pre-cultivation, *E. coli DH5a* from a selective plate (35 g/L LB-Agar medium supplemented with kanamycin) was transferred to 250 mL shake flask containing 62.5 mL of Luria-Bertani (LB) culture medium. The growth occurred at 37 ºC and 250 rpm, until the cell suspension reached an optical density (OD) at a wavelength of 600 nm (OD_{600}) of 0.3-0.4. These cells were used to prepare competent cells for heat shock method. For this purpose, 50 mL aliquots of cell suspension were centrifuged at 5000 rpm for 10 minutes at 4 ºC. The medium was removed from the cell pellets and each pellet was ressuspended in 12.5 mL of ice-cold 100 mM $MgCl_2$. The cells were recovered again by centrifugation at 4000 rpm for 10 minutes at 4 ºC and ressuspended in 50 mL of ice-cold 100 mM $CaCl_2$. The cell suspension was maintained on ice for at least 20-30 minutes. After this, the bacterial culture was centrifuged at 4000 rpm for 10 minutes at 4 ºC and the pellet was ressuspended in 1 mL of ice-cold 85 mM $CaCl_2$ containing ice-cold 15 % (w/v) glycerol for each 50 mL of original culture. Then, 100 µL of competent cells were pipetted into separated Eppendorfs. The plasmids pBHSR1-RM-pre-miR-9/29b were introduced into 0.1 mL of competent *E. coli DH5a* cells by the heat shock method. The transformation occurred by thermal shock, using the following conditions: 30 minutes at 4 ºC, 1 minute at 42 ºC and 2 minutes at 4 ºC, using 100 ng of plasmids pBHSR1-RM-pre-miR-9/29b. After the heat shock, 200 µL of medium was added to the transformation mixture and cells were incubated at 37 ºC, 250 rpm for 2 hours to allow the expression of antibiotic resistance gene and to stabilize the bacteria. The cells were then plated in LB-Agar plates with kanamycin (30 µg/mL) and incubated overnight at 37 ºC, until the growth of colonies. Some isolated colonies were transferred into LB medium and grown at 37 ºC, 250 rpm, overnight. From these bacterial cultures, the plasmid pBHSR1-RM-pre-miR-9 was isolated and purified using the NZYMiniprep Kit (NZYtech, Lisbon, Portugal) and digested with Stu*I* and Xba*I* to confirm the presence of the pre-miR-9 sequence. PCR was carried out to confirm the presence of the pre-miR-9 sequence in the vector. The pre-miR-9 sequence cloned into the vector was confirmed by nucleotide sequentiation.

2.2.5. Nucleotide Sequentiation

The pBHSR1-RMplasmid containing pre-miR-9 sequence was sequenced in order to confirm the identity and orientation of the amplicon. The DNA sequencing reaction was carried out following the protocol GenomeLab™ Dye Terminator Cycle Sequencing with Quick Start Kit for GenomeLabTM GeXP sequencer (250 S. Kraemer Boulevard Brea, CA 92821). Sequence data was analyzed using GenomeLab system Beckman Coulter version 10.2 software.

2.2.6. *E. coli DH5a* culture and production of pre-miR-9/29b

E. coli DH5α cells previously transformed by heat-shock with plasmid pBHSR1-RM containing the sequence of human pre-miR-9/29b were used in this study for recombinant pre-miR-9/29b production. These cells were grown at 37 ºC, overnight in LB-Agar medium plates supplemented with 30 µg/mL kanamycin. Then, *E. coli DH5a* colonies were transferred into

pre-fermentation medium and incubated at 37 ºC, 250 rpm. The terrific broth medium (12 g/L tryptone, 24 g/L yeast extract, 0.017 M KH_2PO_4, 0.072 M K_2HPO_4 and 4 ml/L glycerol) supplemented with 30 µg/mL kanamycin was used for the pre-fermentation and fermentation in shake flasks. Cell growth was monitored by measuring the OD_{600}. Once the pre-fermentation growth reached an OD_{600}~2.6 (exponential phase), a volume of culture was transferred into fermentation media and incubated at 37 ºC, 250 rpm. The volume transferred from pre-fermentation to fermentation was calculated in a way that the optical density of cells in the beginning of the fermentation would be of approximately 0.2 according to equation (1).

$$V_{\text{from pre-fermentation}} = \frac{V_{\text{fermentation}} \times OD_{\text{fermentation}}}{OD_{\text{pre-fermentation}} - OD_{\text{fermentation}}} \quad (1)$$

OD was measured with Pharmacia Biotech Ultrospec 3,000 UV/Visible Spectrophotometer (Cambridge, England). At the end of fermentation, cells were harvested by centrifugation (4,000 g, 15 minutes, 4 ºC) and stored at -20 ºC until use.

2.2.7. RNA Extraction from *Escherichia coli DH5a*

RNA extraction was carried out based on the guanidinium thiocyanate-phenol-chloroform RNA isolation protocol [95]. The *E. coli DH5a* pellets (from 50 mL of culture medium) were thawed and ressuspended with 0.8 % sodium chloride solution. The suspensions were centrifuged at 6,000 g, 4 ºC for 10 minutes and the supernatant was discarded. Cell lysis was performed with 5 mL of solution D (4 M guanidine thiocyanate, 25 mM sodium citrate, 0.5 % N-laurosylsarcosine and 0.1 M β-mercaptoethanol) and the lysates were ressuspended by successive pipetting and incubated on ice for 10 minutes. Then, 0.5 mL of 2 M sodium acetate pH 4 (prepared with sodium acetate anhydrous and glacial acetic acid) were added to the tubes, followed by a vigorous mixing and the sequential addition of 5 mL of water-saturated phenol, also followed by vigorous mixing and 1 mL of chloroform/isoamyl alcohol (49:1) mixed thoroughly, until two immiscible phases were obtained. Suspensions were incubated on ice for 15 minutes and centrifuged at 10,000 g, 4 ºC for 20 minutes. The supernatants were carefully pipetted into new lysis tubes and 5 mL of isopropanol were added to each tube for RNA precipitation, followed by a centrifugation (10,000 g, 4 ºC for 20 minutes). The supernatants were discarded and the pellets were ressuspended with 1.5 mL of solution D by vortexing and precipitated with isopropanol (same volume of solution D). After the centrifugation at 10,000 g, 4 ºC for 10 minutes, the resulting pellet was washed with 75 % ethanol (in DEPC water), incubated at room temperature for 15 minutes and centrifuged at 10,000 g, 4 ºC for 5 minutes. The pellets were dried at room temperature for 15 minutes and finally ressuspended with 1mL of 0.05 % DEPC-treated water. RNA concentrations were determined using a

NanoPhotometer spectrophotometer (IMPLEN, United Kingdom). The samples were stored at -80 ºC.

2.2.8. Arginine Affinity Chromatography

The recombinant pre-miR-9 and pre-miR-29 samples obtained after small RNA extraction from *E. coli DH5a* were selectively separated by arginine affinity chromatography, using an epoxy arginine monolith. The chromatographic experiments were performed in an AKTA Avant system with UNICORN^{TM} 6.1 software (GE Healthcare, Sweden). To perform the assays, a 1 mL/min flow rate was used and the absorbance of the eluate was continuously monitored at 260 nm. In the stepwise with three steps assay, the arginine monolithic disk was differently equilibrated with 0.98 M NaCl in 10 mM Tris-HCl buffer (pH 6.5) for pre-miR-9 assays and 0.94 M NaCl in 10 mM Tris-HCl buffer (pH 6.5) for pre-miR-29 assays. The samples were injected into a 100 µL loop and eluted by using an increasing NaCl stepwise gradient. After elution of unbound species with the initial equilibrium buffer, the second gradient for the pre-miR-9 isolation was 1.12 M NaCl in 10 mM Tris-HCl buffer (pH 6.5) and in the case of the pre-miR-29 isolation the gradient used was 1.12 M NaCl in 10 mM Tris-HCl buffer (pH 6.5). Afterwards, for the elution of pre-miR-9 the gradient used was 1.62 M NaCl in 10 mM Tris-HCl buffer (pH 6.5) and for the elution of pre-miR-29 the gradient used was 1.6 M NaCl in 10 mM Tris-HCl buffer (pH 6.5). In the stepwise gradient with two steps, the arginine monolithic disk was differently equilibrated with 1 M NaCl in 10 mM Tris-HCl buffer (pH 6.5) for pre-miR-9 assays and 1 M NaCl in 10 mM Tris-HCl buffer (pH 6.5) for pre-miR-29 assays. The samples were injected into a 100 µL loop and eluted by using an increasing NaCl stepwise gradient. After elution of unbound species with the initial equilibrium buffer, the last gradient for the pre-miR-9 isolation was 1.6 M NaCl in 10 mM Tris-HCl buffer (pH 6.5) and in the case of the pre-miR-29 isolation the gradient used was 1.6 M NaCl in 10 mM Tris-HCl buffer (pH 6.5). The pooled fractions were concentrated and desalted with Vivaspin 5,000 MWCO concentrators (Vivascience) and the samples were stored at -80 ºC for further analysis.

2.2.9. Polyacrylamide Gel Electrophoresis

Denaturing urea polyacrylamide gel electrophoresis was performed to analyze the integrity and to identify the RNA species present on the collected fractions. Samples were denatured with a formamide solution (97.5 % formamide, 0.3 % bromofenol, 10 mM EDTA at pH 7.5) at 55 ºC for 5 minutes and denatured conditions were kept in the gel due to the presence of 8 M urea. 10 µL from the concentrated peaks were then resolved into a 10 % polyacrylamide TBE-urea gel that was carried out in Tris-Borate-EDTA (TBE) buffer (0.84 M Tris-base, 0.01 M EDTA, 0.89 M boric acid, pH 8.3) at 150 V. The gel was stained with GreenSafe Premium (100 µL/L) for 15 minutes and the results were revealed under UV light in an UVITEC Cambridge Fire-reader XS D-56-26LM system (Cambridge, UK).

2.2.10. Protein quantification

A very important step is the verification of protein contamination of the RNA samples. Thus, the protein quantification in each sample was performed using Bicinchoninic Acid (BCA) protein assay kit from Pierce (Thermo Fisher Scientific Inc.), according to manufacturer's instructions. First, a calibration curve was prepared with bovine serum albumin (BSA) standards with concentrations ranging from 0 to 150 µg/mL (Figure 8). Afterwards, 10 µL of each standard, pre-miR-9 and pre-miR-29 samples were pipetted into each *well* with 200 µL of BCA reagent, which were incubated at 60 ºC for 30 minutes. The absorbance values were measured at 570 nm in microplate reader.

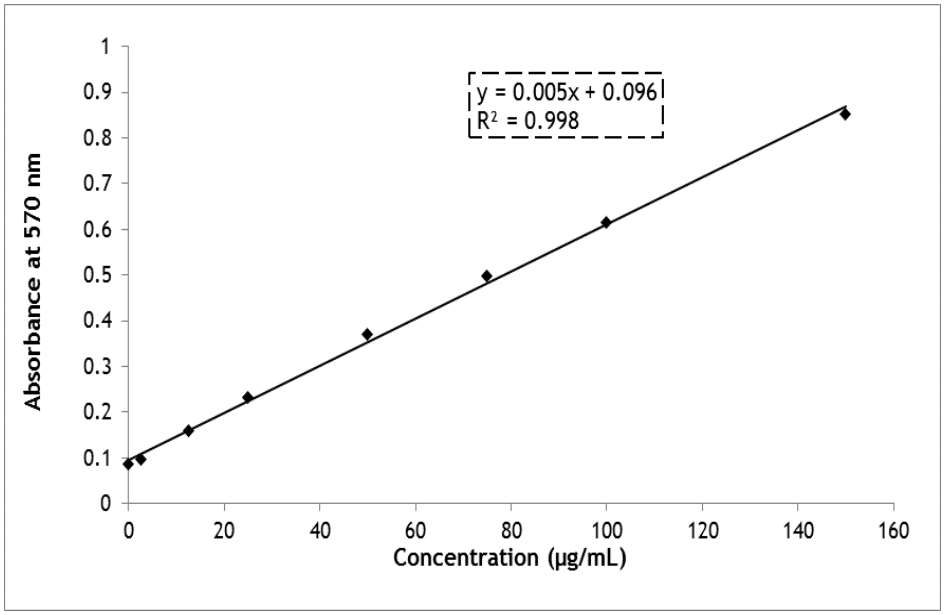

Figure 8 - Calibration curve for protein quantification. Bovine serum albumin (BSA) standards were prepared with concentrations ranging from 0 to 150 µg/mL.

2.2.11. Genomic DNA quantification

The concentration of gDNA in the purified samples was evaluated by real-time qPCR in an iQ5 Multicolor Real-Time PCR Detection System (Bio-Rad). Specific primers (Forward-5'-ACACGGTCCAGAACTCCTACG-3' and Reverse -5'-CCGGTGCTTCTTCTGCGGGTAACGTCA-3') were used to amplify a 181 base pair (bp) fragment of the 16S rRNA *E. coli* gene. PCR amplicons were quantified by following changes in fluorescence of the DNA binding dye SYBR Maxima®Green/Fluorescein qPCR Master Mix (Thermo Fisher Scientific Inc.). The calibration curve to achieve the gDNA concentration was constructed by serial dilutions of the *E. coli DH5a* gDNA sample (purified with the Wizard® Genomic DNA Purification kit, Promega), in the range of 0.005 to 50 ng/µL (Figure 9).

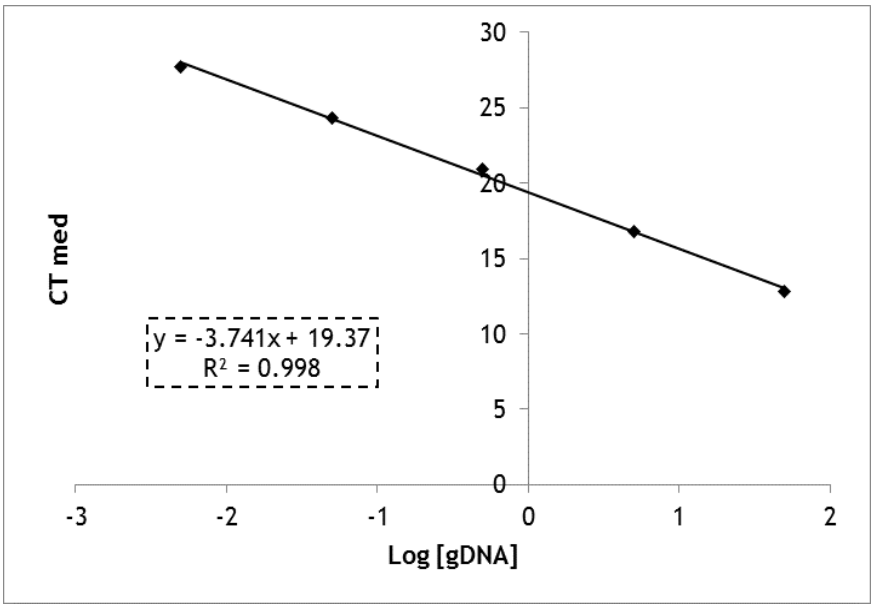

Figure 9 - Calibration curve for gDNA quantification. The curve was constructed by serial dilutions of E. coli DH5α gDNA sample (purified with the Wizard® Genomic DNA Purification kit, Promega), in the range of 0.005 to 50 ng/µL.

2.2.12. Chitosan nanoparticles: formulation and pre-miR-9 and pre-miR-29 encapsulation

The pre-miR-9/29b-loaded polyplexes were formulated using the method of simple complexation through electrostatic interactions that occur between molar concentrations of positive charge, present in the protonated amine groups (N) of chitosan, and the negative charge of the phosphate groups (P) of RNA backbone, as described by Pereira and co-workers [79].

The pre-miR-9/29b (final concentration of 2 µg/mL) and chitosan (concentration of 10 mg/mL) stock solutions were prepared in sodium acetate buffer (0.1 M sodium acetate/0.1 M acetic acid, pH 4.5). Briefly, the pre-miR-9/29b-loaded polyplexes were obtained by dropwise addition of 100 ml of chitosan solution to the pre-miR-9/29b solutions (400 µL), under stirring during 1 minute. The formulated polyplexes were incubated at room temperature for 30 minutes and then pelleted by centrifugation at 15000 g for 20 minutes.

2.2.13. N2a695 cell culture and transfection with CS-pre-miR-9/29b

To access the effects of the studied pre-miRNAs *in vitro*, N2a695 cells were chosen because in these cells there is a constitutive endogenous human BACE1 expression, enabling greater sensitivity for detecting pre-miR-29b induced changes in the human BACE1 expression at post-transcriptional level. First, N2a695 cells at passages 13-27 were cultured in the following medium: 1:1 mixture of Dulbecco's modified Eagle's medium (DMEM) and OptiMEM supplemented with 5 % (wt/vol) heat-inactivated fetal bovine serum (FBS) and 1 % (wt/vol) penicillin-streptomycin. Then, N2a695 cells were seeded in 12-well plates at a density of 2×10^4 cells/well in 1.5 mL of complete medium. Cells were left to grow until 50 to 60 % of

confluence, after which the culture medium was replaced by FBS-free culture medium and kept for 12 hours in growth optimal conditions. For the present study, cells were transfected with 8.72 nM recombinant pre-miR-9, 8.72 nM recombinant pre-miR-29, 9.9 nM unrelated RNA (5'-UGUGCAAAUCUAUGCAAAACUGA-3') and 9.9 nM scrambled miRNA (5'-UUCUCCGAACGUGUCACGUTT3'; 3'-TTAAGAGGCUUGCACAGUGCA-5') using chitosan. The non-transfected cells were used as negative control. After 6 hours of transfection, the culture medium was replaced by fresh medium supplemented with 1 % FBS and 1 % antibiotic, to allow the cells to remain metabolically active, expressing human BACE1 [96]. Each cell group was performed in triplicate and cells were harvested 48 and 72 hours after transfection. All media were prepared at pH 7.4 and cell growth conditions were 37 ºC and 5 % CO_2.

2.2.14. Total intracellular RNA extraction from N2a695 cell line

Total RNA was extracted from the N2a695 cells using TRIzol reagent (Invitrogen,Carlsbad, CA, USA), according to the protocol provided by the manufacturer. Briefly, 300 µL TRIzol were added to each *well* of the plaque and then, cells were pipetted into separated eppendorfs and incubated at room temperature for 5 minutes. To each eppendorf, 60 µL of chloroform was added and incubated at room temperature for 10 minutes. After incubations, cells were centrifuged at 12,000 g and 4 ºC for 15 minutes. After centrifugation, the aqueous phase was transferred to new tubes, and the RNA was precipitated with isopropanol at -20 ºC. The mixture was incubated at room temperature for 10 minutes, after which were centrifuged at 12,000 g and 4 ºC for 10 minutes. The resultant supernatant was discarded and 160 µL of ethanol 75 % were added to each precipitate to wash the RNA and these were centrifuged at 7,500 g and 4 ºC for 5 minutes. The pellets were recovered and air dried at room temperature and ressuspended with 10 µL of 0.05 % DEPC-treated water. To verify the integrity and purity of the RNA, an agarose gel electrophoresis was performed. Total RNA samples were quantified and their purity evaluated (260/280 nm ratio) using a NANOPhotometer.

2.2.15. cDNA synthesis

Total RNA extracted from N2a695 cells was treated with DNase I to eliminate gDNA contamination. Complementary DNA (cDNA) synthesis was performed using RevertAid First Strand cDNA Synthesis Kit (Thermo Fisher Scientific Inc.), according to manufacturer's instructions. To 1 µg of total RNA of samples collected after the transfection, 1 µL of Random Hexamer primer was added, followed by the addition of nuclease-free water up to 12 µL of reaction volume. The mixture was incubated at 65 ºC for 5 minutes on Thermocycler Professional basic gradient purchased from Biometra (Germany). To the previous mixture the following reagents were sequentially added: 4 µL of 5X Reaction Buffer, 1 µL of RiboLock RNase Inhibitor (20 U/µL), 2 µL of 10 mM dNTP Mix and 1 µL of RevertAid M-MuLV Reverse Transcriptase (200 U/µL). The preparation was mixed and briefly centrifuged, after which was incubated at 25 ºC for 5 minutes followed by incubation at 42 ºC for 60 minutes. The reaction was stopped by incubation at 70 ºC for 5 minutes.

2.2.16. Quantification of expression of BACE1 and PSEN mRNAs by RT-qPCR

For quantitative analysis of the expression of the mRNA of BACE1 and PSEN, RT-qPCR amplification of synthesized cDNA was performed using the Maxima® SYBR Green/Fluorescein qPCR Master Mix (2X) (Thermo Fisher ScientificInc.) in an IQ5 Cycler from BioRad. RT-qPCR reaction was prepared containing 10 µL of Maxima® SYBR Green/Fluorescein qPCR Master Mix (2X), 1.2 µL of each 25 µM forward and reverse primers, 2 µL cDNA and nuclease-free water up to a final volume of 20 µL per reaction, under the following conditions: 95 ºC for 5 minutes for initial denaturation, followed by 40 cycles of 30 seconds at 95 °C, 30 seconds at 62 °C and 30 seconds at 72 °C. Primers used for the amplification of BACE1 were: forward primer 5'-AGACGCTCAACATCCTGGTG-3' and reverse primer 5'-CCTGGGTGTAGGGCACATAC-3'; for the amplification of glyceraldehyde-3-phosphate dehydrogenase (GAPDH) forward primer 5'-TGACGTGCCGCCTGGAGAAA-3' and reverse primer 5'-AGTGTAGCCCAAGATGCCCTTCAG-3' were used, and for the amplification of PSEN forward primer 5'-GAGGAAGACGAAGAGCTGACA-3' and reverse primer 5'-GAAGCTGACTGACTTGATGGTG-3' were used. RT-qPCR efficiencies were calculated from the given slopes with MyIQ 2.0 software (BioRad). The relative quantification of BACE1 and PSEN expression was based on the comparative threshold cycle (C_T) method in which the amount of the target was determined to be $2^{-(\Delta CT\ target\ -\ \Delta CT\ calibrator)}$, normalized to levels of GAPDH and relative to the untreated control cells. Each sample was run in triplicate, and threshold cycle (C_T) values were averaged from the triplicate. The final data were averaged from three separately conducted experiments.

Chapter III

Results and Discussion

3.1. pBHSR1-RM-pre-miR-9 plasmid construction

The first aim of this study was the construction of pBHSR1-RM vectors containing the pre-miR-9 sequence. The pre-miRNA was produced and purified instead of the mature miRNA, since it is described that the recognition and processing within the cell is more efficient. Furthermore, different pre-miRNA structural characteristics, including the single chain with ~80 nucleotides of which some are unpaired in the 3'overhang, will eventually facilitate its purification, as previously reported by Pereira and collaborators [80, 96]. The pre-miR-29 sequence had been previously cloned into the plasmid DNA (pDNA) vector pBHSR1-RM by Pereira and co-workers [80]. So, the following step was to clone the pre-miR-9 sequence into the pBHSR1-RM vector. For this, the previously constructed pBHSR1-RM-pre-miR-29 vector was digested with *StuI* and *XbaI* enzymes to cut off the pre-miR-29 sequence from the vector. Then, the pre-miR-9 sequence was amplified by PCR with primers containing two appropriate restrictions sites for *StuI* and *XbaI* for directional cloning. Then, the DNA fragment containing pre-miR-9 sequence was cloned into the pBHSR1-RM vector, previously digested with the same restriction enzymes.

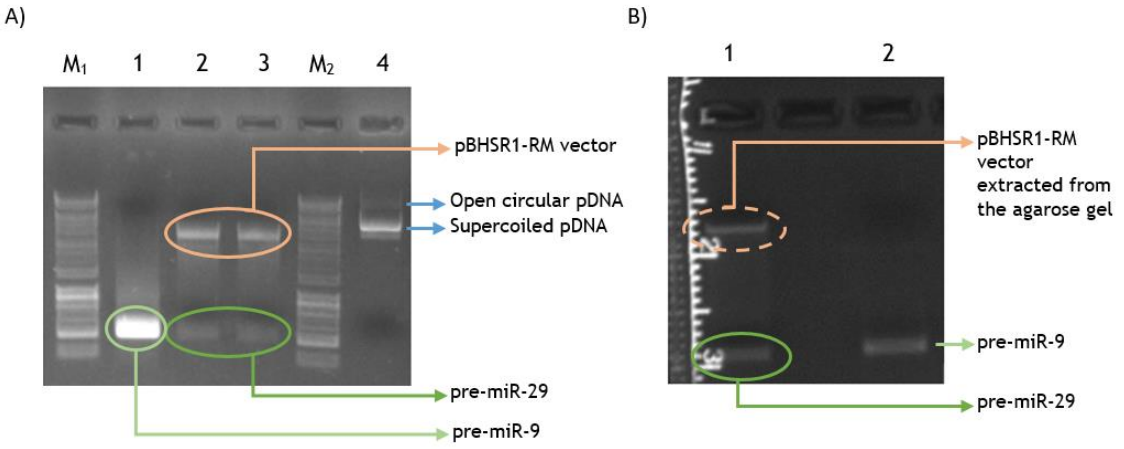

Figure 10 - Plasmid pBHSR1-RM and pre-miR-9 digestions. A) Agarose electrophoresis with the digested pre-miR-9 sequence (lane 1) and the plasmid pBHSR1-RM vector containing the pre-miR-29 sequence (lanes 2 and 3) after digestion with *StuI* and *XbaI* restriction enzymes. Plasmid pBHSR1-RM vector (lane 4) was also pipetted into the agarose gel for comparison. Lanes M_1 and M_2 correspond to the molecular weight markers (200-10 000 bp). B) Agarose electrophoresis with the digested plasmid pBHSR1-RM vector which previously contained the pre-miR-29 sequence (lane 1) and the pre-miR-9 sequence (lane 2) digested with *StuI* and *XbaI* enzymes.

In the Figure 10A (lanes 2 and 3) is represented the digestion of the pBHSR1-RM-pre-miR-29 vector with restriction enzymes, to evaluate the presence of the cloned pre-miR-29

sequence, and confirm the predicted molecular size of the sequence. As a means of comparison the non-digested pBHSR1-RM-pre-miR-29 plasmid, presenting the open circular and supercoiled isoforms, was submitted to the same electrophoresis as shown in Figure 10A (lane 4) being verified a slight increase in molecular weight relatively to the vector in lanes 2 and 3 of the same figure. Afterwards, the resulting fragments from the pBHSR1-RM-pre-miR-29 digestion were separated from each other by a 0.8 % agarose electrophoresis as shown in Figure 10B (lane 1). The electrophoretic analysis of the PCR product obtained from the amplification with the specific primers for pre-miR-9 Figure 10B (lane 2) showed one band corresponding to the size of the gene of interest, which presents a molecular weight comparable to the pre-miR-29 sequence. The portion of agarose gel containing the vector (free from pre-miR-29 gene) was cut off as indicated in Figure 10B (lane 1) and the vector was purified using the PCR clean-up, gel extraction kit. Finally, the pre-miR-9 sequence was cloned into the pBHSR1-RM vector.

3.2. *E. coli DH5a* transformation and pBHSR1-RM-pre-miR-9 plasmid amplification and sequencing

In this study, recombinant pre-miR-9 and pre-miR-29 were produced in a genetically modified organism, *E. coli DH5a*, harboring recombinant plasmids pBHSR1-RM-pre-miR-9 or pBHSR1-RM-pre-miR-29. This bacterial strain was chosen as host because it allows the recombinant RNA production [97], it is easy to manipulate genetically and presents a short duplication time, within which the interest molecules are produced [98]. Competent *E. coli DH5a* cells were transformed by heat shock, which allows the intracellular access of the plasmid DNA through this gram-negative type membrane pores. Afterwards, transformed bacteria were plated in the LB-Agar medium supplemented with kanamycin. The presence of kanamycin in the medium provides a selective strategy to distinguish transformed and non-transformed bacteria because the pBHSR1-RM plasmid contains a sequence that is responsible for the induction of the kanamycin resistance mechanism. In this way, isolated bacterial colonies growing in the plate possess this resistance mechanism and were much probably successfully transformed. Nevertheless, more accurate analysis is necessary to confirm the correct transformation. The isolated colonies present in the plate were separately ressuspended in LB culture medium supplemented with kanamycin, in order to promote their growth. When the desired cellular density was achieved, the plasmid pBHSR1-RM-pre-miR-9 of each fermentation, corresponding to one-single initially identified colony, was isolated and purified using the NZYMiniprep Kit.

After plasmid pBHSR1-RM-pre-miR-9 isolation and purification with NZYMiniprep Kit the resultant plasmid suspensions were analyzed by 1 % agarose gel electrophoresis. As it may be verified in Figure 11, the different isoforms of the pDNA were observed including open circular and supercoiled isoforms.

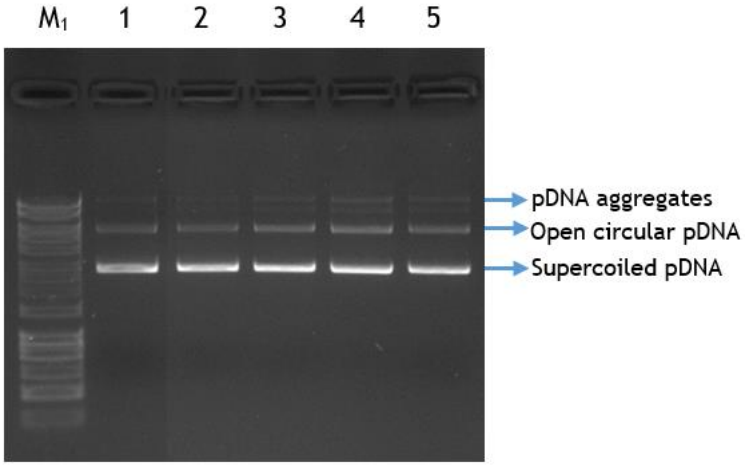

Figure 11 - Agarose electrophoresis with the purified plasmids of pBHSR1-RM-pre-miR-9. Plasmids of pBHSR1-RM-pre-miR-9 produced in transformed *E. coli DH5a* (lanes 1 to 5). Lane M_1 corresponds to the molecular weight marker (200-10 000 bp). Lanes 1 to 5 correspond to the analysis of the different isolated colonies fermentations.

A PCR was carried out with specific primers of pre-miR-9 sequence (forward primer 5'-GGGGTTGGTTGTTATCTTTGG-3' and reverse primer 5'-TGGGGTTATTTTTACTTTCG-3'), in order to verify if the sequence of interest (pre-miR-9) was present in the recombinant pBHSR1-RM-pre-miR-9 plasmid and confirm the successful *E. coli DH5a* transformation.

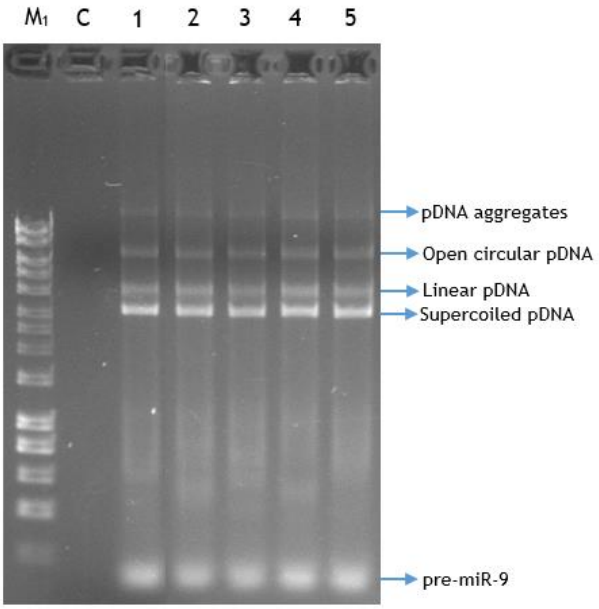

Figure 12 - Agarose electrophoresis of PCR reactions conducted with primers of pre-miR-9 in different recombinant pBHSR1-RM-pre-miR-9 plasmids. Recombinant pBHSR1-RM-pre-miR-9 plasmids were extracted from transformed *E. coli DH5a* cells. Samples 1 to 5 (lanes 1 to 5) had the pre-miR-9 sequence successfully amplified. Lane M_1 corresponds to the molecular weight marker (200-10 000 bp) and lane C corresponds to the negative control of the PCR.

The PCR products were analyzed by 1 % agarose electrophoresis as shown in Figure 12, where it was verified that samples 2 and 3 (lanes 4 and 5) were false positive colonies, since the

pre-miR-9 was not amplified, unlike samples 1 (lane 3) and 4-7 (lanes 6-9) which contained the pre-miR-9 sequence.

3.2.2. Nucleotide sequentiation of transformed *E. coli DH5a*

To effectively confirm the identity, orientation and frame of the extracted pBHSR1-RM vector which contained the pre-miR-9 sequence, the vector was sequenced using Forward primer pBHSR1-RM_StuI_premiR_511Fw 5' - CGAGGCCTAGGAAGCTGGTTTCATATGGTGGTTTAGATTTAAATAGTGATTGTCTAGCACATTTGAAAT CAGTGTTCTTGGGGGATCATACCGCTGTCAGCCGTGCAAG- 3' and Reverse primer pBHSR1-RM_XbaI_820Rv 5' - CATCTAGAGCTCATGCCCTTGAGATCGGCC – 3'. The nucleotide sequencing of a pBHSR1-RM-pre-miR-9 plasmid sample was carried out and it was verified that the cloned sequence corresponds to the pre-miR-9 gene, as demonstrated in Figure 13.

Figure 13 - Sequencing of the recombinant plasmid pBHSR1-RM-pre-miR-9. The sequence highlighted in blue corresponds to the sequence that will originate the pre-miR-9. The sequence in yellow refers to the recognition sequence of restriction enzyme *StuI* and in green is highlighted the recognition sequence of *XbaI* restriction enzyme. These two enzymes cut between the two underlined bases of the respective recognition sequences.

3.3. Recombinant pre-miR-9 and pre-miR-29 production in *E. coli DH5a*

In this project it was also tried to develop a new strategy to biosynthesize pre-miRNAs using the bacterium *E. coli*, resulting in the improvement of RNA production and quality with a less time-consuming and expensive procedure. Thus, *E. coli DH5a* cells transformed either with pBHSR1-RM-pre-miR-9 or pBHSR1-RM-pre-miR-29 plasmids were separately cultivated, allowing the replication of the plasmids and consequently the expression of the recombinant miRNAs (pre-miR-9 and pre-miR-29). As expected, *E. coli* was able to grow at 37 ºC (Figure 14), and the experimental conditions applied promoted the bacterium growth until reaching optical densities of 5.392±0.109 after 6 hours of cultivation as depicted in Figure 14.

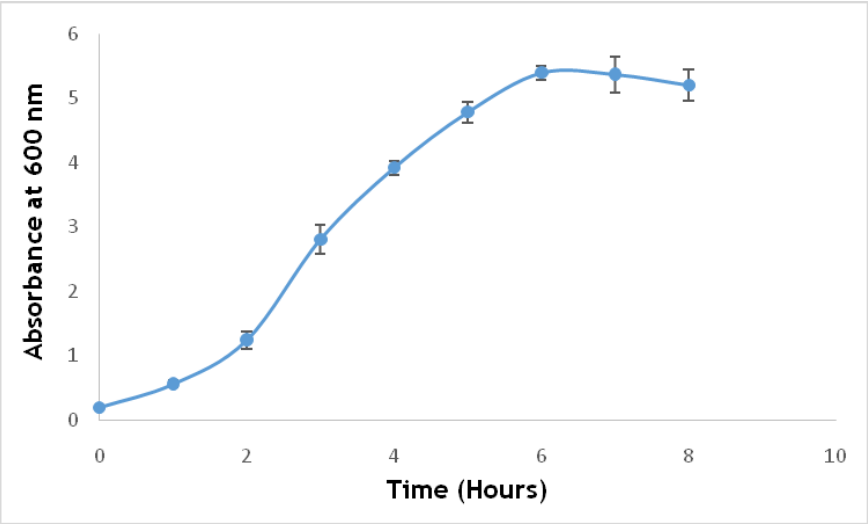

Figure 14 - Representative growth curve of *E. coli DH5a* bearing the pBHSR1-RM-pre-miR-9 or pBHSR1-RM-pre-miR-29. Fermentation was carried out for 8 hours at 37 ºC and 250 rpm. Growth occurred for 6 hours after which it started to decrease.

To elucidate the relation between cell growth and the production of pre-miR-9/29, the intracellular nucleic acids were isolated and analyzed at various time points of the culture. To accomplish this, the cells were recovered by centrifugation and the total *E. coli DH5a* RNA containing pre-miR-9 or pre-miR-29 was extracted by the acid guanidinium thyocianate-phenol-chloroform method [95] and the resultant pellets were ressuspended in DEPC water. A 1 % agarose gel electrophoresis was carried out to verify if these samples were contaminated with gDNA. Figure 15 shows an agarose electrophoresis and its analysis revealed the presence of bands corresponding to small RNAs and also faint bands with higher molecular weights, corresponding to the 23S and 16S ribosomal RNA (rRNA), however there was no contamination with gDNA [80].

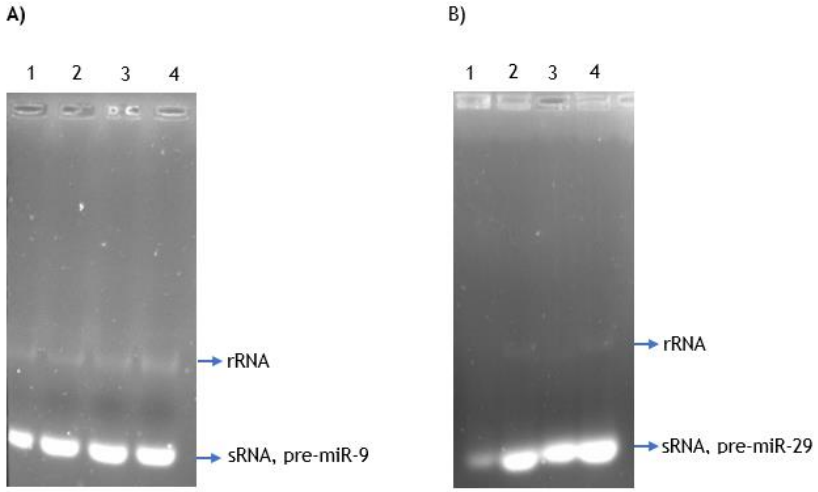

Figure 15 - Agarose electrophoresis of total RNA extraction. A) Agarose electrophoresis of total RNA extraction containing recombinant pre-miR-9 from *E. coli DH5a*. Lanes 1-4 correspond to samples 1-4 respectively. B) Agarose electrophoresis of total RNA extraction containing recombinant pre-miR-29 from *E. coli DH5a*. Lanes 1-4 correspond to samples 1-4 respectively.

In addition, several classes of sRNA are present in sharp bands of low molecular weight (below 500 bp), corresponding to transfer RNAs (typically 73 to 94 bp), 6S RNA (184 bp), and pre-miR-9/29 (110 bp) [80]. Also, the RNA concentration was determined by spectrophotometric analysis, measuring the absorbance at 260 and 280 nm. The 260/280 ratio was also determined, which is an indication of the purity of each sample, with a ratio of 2 being achieved, which is often characteristic of a pure RNA preparation [99].

3.3.1. pre-miR-29, proteins and genomic DNA content during *E. coli* DH5α fermentation

The time-course profiles of production of pre-miRNA were evaluated after the synthesis of cDNA from each extracted RNA fraction followed by RT-qPCR analysis using a specific probe, to detect the pre-miR-29 sequence. This analysis enables a more accurate quantification of the pre-miRNA present in each sample of *E. coli DH5α*. The maximum level of production of the pre-miR-29 was observed at 6 hours of cultivation with 3047±323.8 µg/L of culture (Figure 16). As can be seen by comparing Figure 16 with Figure 14, the production of pre-miR-29 increased with the cell growth until 6 hours of fermentation, after which a significant decrease in pre-miR-29 production was observed.

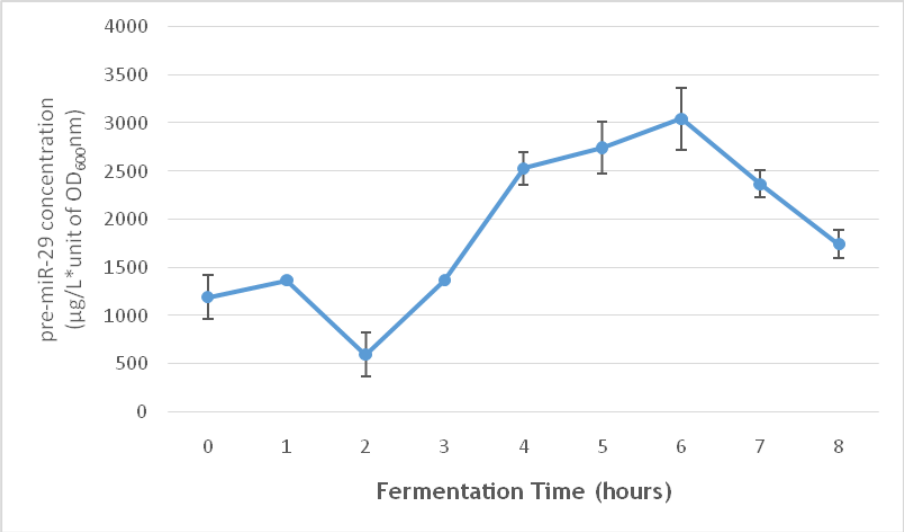

Figure 16 - Time-course profile of pre-miR-29b production in *E. coli DH5a* cultures. Pre-miR-29b levels were measured by quantitative RT-PCR using a specific probe as indicate in Materials and Methods section. Error bars indicate standard deviations calculated form three independent experiments.

Regarding the applicability of this method to obtain recombinant pre-miRNAs, the contamination level should also be assessed and so, the levels of gDNA and proteins were evaluated during the fermentation time. The proteins level in RNA samples was quantified by the micro-BCA method throughout the cultivation time (Figure 17). The results for protein quantification in the RNA fraction revealed that the protein level was high during the first 5 hours of cultivation, with a maximum value of 139.05±6.68 µg/µL at 5 hours (Figure 17).

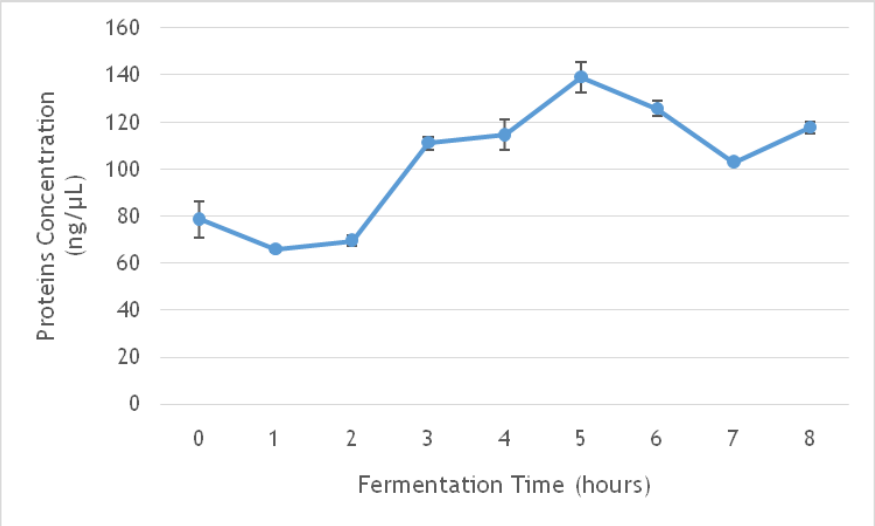

Figure 17 - Proteins concentration (ng/µL) during the *E. coli* DH5α fermentation process.

The time course profile of gDNA along the *E. coli* culture was also determined by quantitative real-time PCR (Figure 18). The gDNA concentration decreased abruptly until 6 hours of fermentation, after which a rapid increase of gDNA is remarkable. This may be attributable to the release of the intracellular components cause by *E. coli DH5α* lysis.

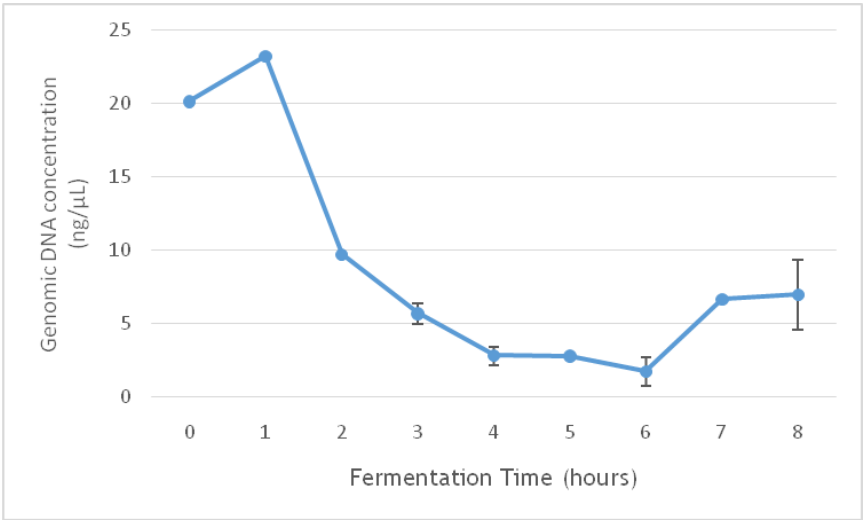

Figure 18 - Genomic DNA concentration (ng/µL) during the *E. coli* DH5α fermentation process.

3.4. Recombinant pre-miR-9 and pre-miR-29 purification by affinity chromatography using arginine monolith

After establishing the recombinant pre-miR-9/29 production process, a purification strategy that allows the recovery of these pure RNAs was the following very important step. To maintain the biological activity of the pre–miR-9 and pre-miR-29, a chromatographic strategy that would keep their native structure would be ideal. To accomplish this, affinity chromatography was employed to selectively purify the target RNAs by exploring distinct interactions between the different species of a total RNA sample (whether containing pre-miR-9 or pre-miR-29) and amino acid ligands. The chromatographic support chosen was an arginine monolithic support. Arginine was used as a biospecific ligand because it is an amino acid that establishes strong interactions with other biological molecules and specially because it is known to be an abundant component of the active centers of PAZ units of the AGO proteins, immediately suggesting a biological role in the interaction with pre-miRNAs [91]. These interactions were explored with the aim of achieving the chromatographic separation of these nucleic acids from a RNA mixture. Monoliths application has risen as means of fast and accurate chromatographic analysis. As explained earlier, affinity chromatography is based mainly on the profiteering of different kinds of interactions such as hydrogen bonding, cation-π interactions, electrostatic and hydrophobic interactions and van der Waals and dipole-dipole forces. Also, electrostatic interactions can be manipulated by changing the ionic strength of the mobile phase, resulting in different elution patterns. Higher concentrations of NaCl salt in the buffer solutions provide higher ionic strength, which allows the manipulation of the electrostatic interactions between the mobile phase (buffer solutions through the monolith) and the RNA species injected onto the system. So, with higher ionic strength it is achieved the RNA elution, and when the NaCl concentration is lower the interactions between the RNA species and the monolith arginine ligands are favored and higher retention is achieved. These techniques were exploited and the most relevant results are described below. All samples injections whether possessing pre-miR-9 or pre-miR-29, had a volume of 200 µL and approximately 80 µg of total RNA. The pH of the solutions prepared for the chromatographic experiments was of 6.5, as it was concluded to be optimal in these assays (data not shown).

3.4.1. pre-miR-29 purification

As previously referred the pre-miR-29 was submitted to different purification tests. The strategies include a purification using a stepwise gradient with three steps and a purification by using a stepwise gradient with two steps, both by increasing the ionic strength in the mobile phase. In the following two sections, these strategies will be presented.

3.4.1.1. Stepwise pre-miR-29 purification with three elution steps

Initially, a stepwise gradient with three steps characterized by the increasing ionic strength was attempted as suggested by Pereira and coworkers in a pre-miR-29 purification approach [91]. The first step was planned in order to achieve a substantial retention of the target RNA, eluting the other RNA species. For this, a concentration of 0.94 M NaCl in 10 mM Tris-HCl buffer was chosen so that stronger electrostatic interactions would occur between the arginine ligand and the pre-miR-29, resulting in a higher retention. Under these conditions, a first peak of unbound species was obtained as shown in Figure 19A (peak 1). Secondly, a 1.12 M NaCl concentration in 10 mM Tris-HCl buffer was selected to allow a deeper elution of tRNA species. Finally, 1.6 M NaCl in 10 mM Tris-HCl buffer was applied for pre-miR-29 elution. Unlikely the strategy adopted by Pereira and coworkers, where the pre-miR-29 recovery was stablished for the second gradient step [91], in the present work this recovery was performed in the last peak, obtained in the third gradient step (Figure 19A, peak 3). Figure 19A shows the chromatographic profile obtained after the injection of sRNA preparation in the arginine monolithic support.

A)

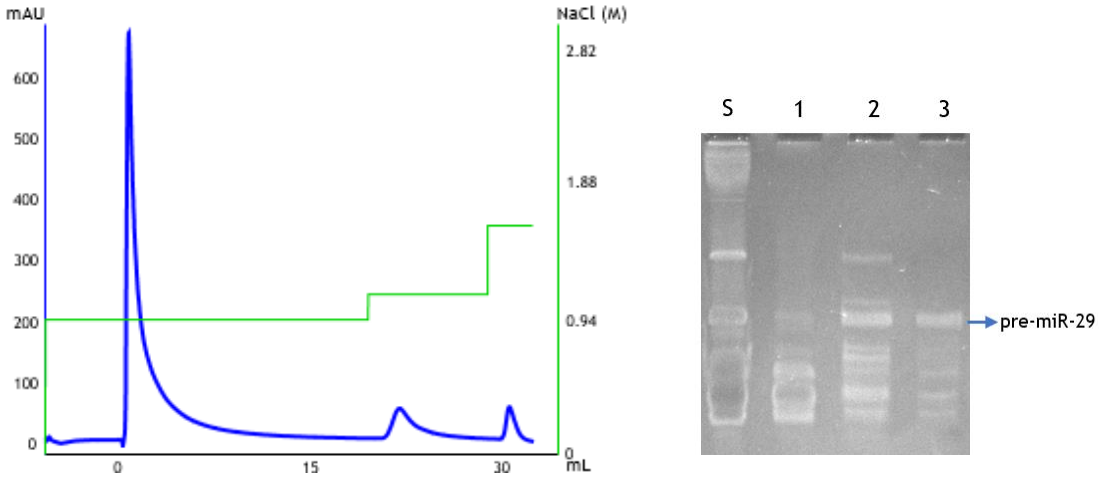

Figure 19 - Stepwise pre-miR-29 purification with three elution steps. A) Chromatographic profile of RNAs elution with arginine monolith. Chromatography was carried out at 1 mL/min by increasing NaCl concentration in a stepwise gradient: 0.94 M NaCl in 10 mM Tris-HCl buffer, 1.12 M NaCl in 10 mM Tris-HCl buffer, 1.6 M NaCl in 10 mM Tris-HCl buffer (pH 6.5). B) Polyacrylamide gel electrophoresis of samples collected from chromatographic assay. Fractions from peaks 1, 2 and 3 are represented in lanes 1, 2 and 3 respectively. Lane S represents the RNA sample injected onto the monolith disk.

The recovery of pre-miR-29 in the last step of the gradient (peak 3) of Figure 19A was considerable and the contamination by other RNA species such as tRNA and 6S RNA were negligible, as noted in lane 3 of Figure 19B. As it can be verified in Figure 19B (lane 1), in the first gradient step some pre-miRNA was eluted with 0.94 M NaCl in 10 mM Tris-HCl. Regarding the second gradient step, it can be seen from Figure 19B (lane 2) that some of the RNA species that were not eluted in the first step, because of the higher retention conditions, were later eluted with 1.12 M NaCl in 10 mM Tris-HCl buffer. Comparatively to the study

carried out by Pereira and co-workers on the pre-miR-29 purification from a total sRNA mixture with arginine affinity chromatography, the first NaCl concentration applied to the sample (Figure 19A, peak 1) allowed the elution of a substantial amount of tRNA species [91]. This suggests that the present strategy also explores the interactions intended in the affinity chromatography. However, there is a main difference between this process and the one previously reported. In previous works the pre-miR-29 was collected in the second gradient step with intermediate NaCl concentration [91], after which the remaining contaminant RNA species were eluted by increasing NaCl concentration. In our study the best pre-miR-29 recovery step changed to be the third step (Figure 19A, peak 3), with higher NaCl concentration (Figure 19B, lane 3). The significant differences between the results of these two studies were caused by the conditions used along the processes, namely the NaCl buffer gradient used and the pH of the buffer solutions. In the present study, a lower pH (6.5) was used contrarily to the pH used by Pereira and coworkers which was 8.0 [91]. The higher pH value allowed the elution of specific RNA species by using lower salt concentration, which also adds value to this previously reported strategy. Nevertheless, with the present strategy, and the adequate sample desalting, a pure pre-miR-29 was also obtained. As reported by Pereira and co-workers in a study involving the purification of pre-mir-29 by agmatine affinity chromatography, an increase in pH also increases the specificity of the agmatine ligand to the pre-miRNAs, first eluting the other sRNAs (mainly tRNAs) [90]. Even though the agmatine ligand presents higher specificity to the pre-miR-29 than the arginine ligand (because of the absence of the carboxyl group) [90], and consequently higher salt conditions were used for eluting bound species [90]. Analyzing the previously mentioned studies, it can be concluded that the arginine amino acid presented more successful results than the agmatine because a lower concentration of salt in the mobile phase was enough along with the other factors involved (amino acid ligand and pH) to purify the target RNA [90, 91]. This work includes arginine using different conditions and a good purity degree was achieved, although the recovery level was much lower than previously reported by other studies [90, 91] and therefore a different approach was tried.

3.4.1.2. Stepwise pre-miR-29 purification with two elution steps

In chromatography, along with a high purity, a high recovery of the RNA of interest should also be obtained and the next experiment was based in minimizing the loss of pre-miR-29. For this, a two-steps experiment was carried out to find out whether pre-miR-29 recovery would improve. Therefore, the NaCl concentration of the first step was adjusted to 1 M NaCl in 10 mM Tris-HCl buffer, maintaining the conditions of the second step in 1.6 M NaCl in 10 mM Tris-HCl buffer. The strategy used for the first step was chosen to allow a significant elution of the undesired RNA species while at the same time permitting a significant pre-miR-29 retention to be then recovered in the last chromatographic step.

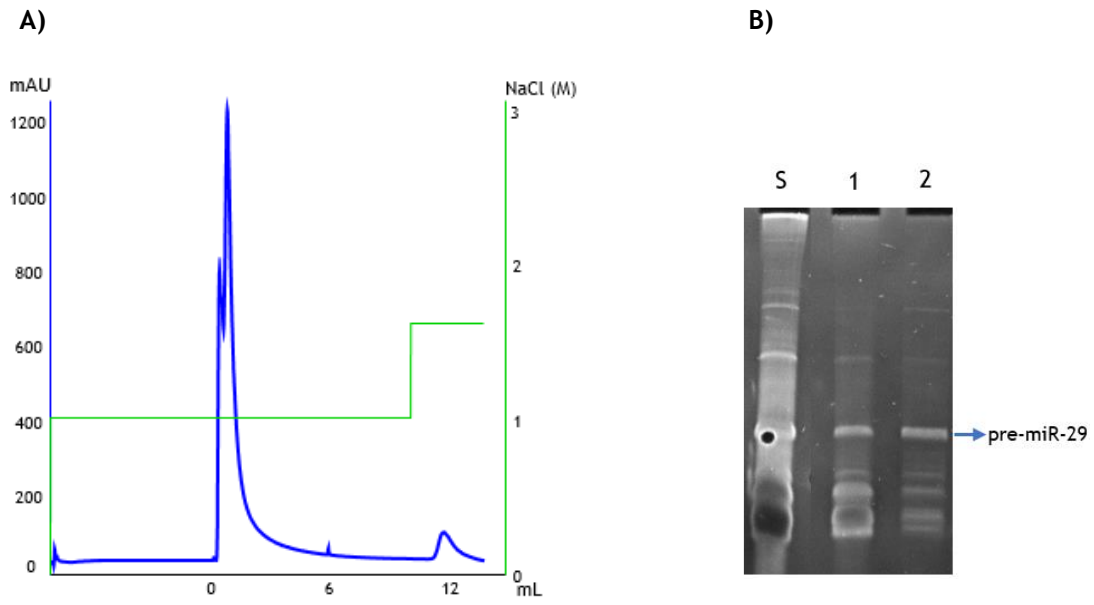

Figure 20 - Stepwise pre-miR-29 purification with two elution steps. A) Chromatographic profile of RNAs elution with arginine monolith. Chromatography was carried out at 1 mL/min by increasing NaCl concentration along the stepwise gradient: 1 M NaCl in 10 mM Tris-HCl buffer, 1.6 M NaCl in 10 mM Tris-HCl buffer (pH 6.5). B) Polyacrylamide gel electrophoresis of samples collected from chromatographic assay. Fractions from peaks 1 and 2 are represented in lanes 1 and 2 respectively. Lane S represents the RNA sample injected onto the monolith disk.

It can be seen from electrophoresis, in Figure 20B, that this chromatographic strategy worked out well when compared with that previously reported (Figure 19B) in that much more pre-miRNA was interacting with the arginine ligands when the second gradient was applied. Nevertheless, the purity of pre-miR-29 present in the fraction collected from peak 2 (Figure 20A) was lower. Indeed, tRNAs, 6S RNA and 5S RNA also had a good affinity for the arginine ligands in these conditions, co-eluting with the target RNA, as it may be seen in Figure 20B (lane 2). In fact, the recovery achieved was comparable to the recovery level reported by Pereira and co-workers in agmatine affinity chromatography [90], although this result is much less satisfactory, in terms of purity, than previously reported results with arginine-affinity chromatography [91].

3.4.2. pre-miR-9 purification

In this section the purification study of pre-miR-9 will be discussed. In the following two subsections, the different strategies that were used to isolate the RNA of interest will be compared. The first strategy presented is the purification of pre-miR-9 with a stepwise gradient containing three elution steps and the second one is the stepwise gradient with two steps.

3.4.2.1. Stepwise pre-miR-9 purification with three elution steps

As in the experiments previously presented involving the purification of pre-miR-29, the initial strategy used for the pre-miR-9 purification was also a stepwise gradient with three steps. This approach was considered because the size of the pre-miR-9 is similar to the size of

pre-miR-29 and this leads to the assumption that the interactions could be similar and therefore the purification process would probably be alike. As the pre-miR-29 had been previously isolated by arginine affinity chromatography with stepwise gradient with NaCl buffer solution [91], it inspired the pre-mir-9 purification aimed in this study. The first gradient step chosen for this strategy was 0.98 M NaCl in 10 mM Tris-HCl buffer for the elution of small weight RNA species (tRNAs) and 6S RNA. In these conditions, pre-miR-9 was expected to interact with the immobilized arginine in the monolith. Then, NaCl concentration was raised to 1.12 M NaCl in 10 mM Tris-HCl buffer for the elution of some additional RNA contaminants. The third and final step of this chromatographic assay was 1.62 M NaCl in 10 mM Tris-HCl buffer, being expected the elution of the highly retained pre-miR-9.

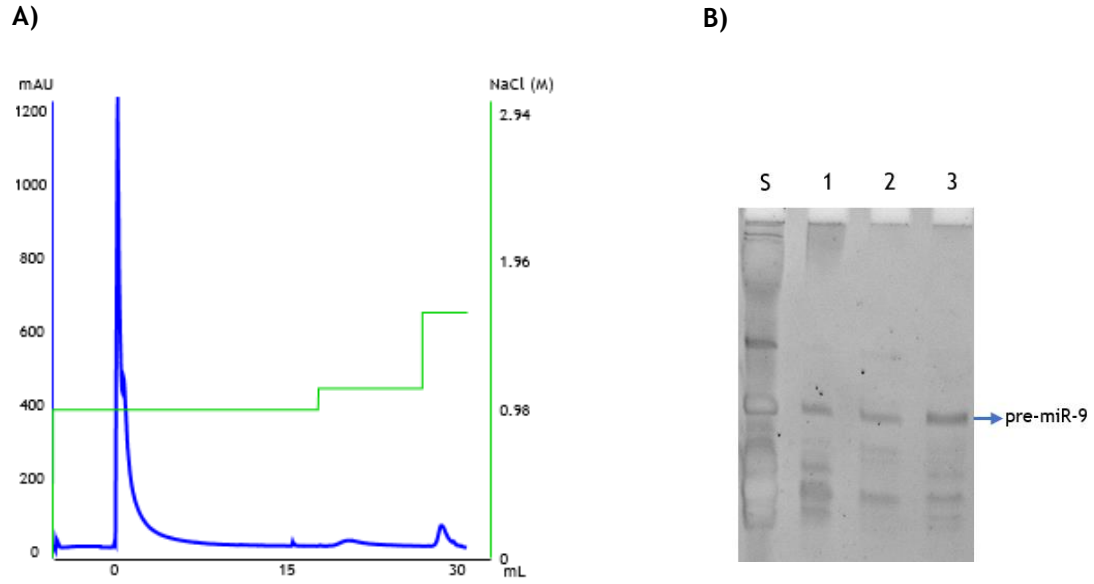

Figure 21 - Stepwise pre-miR-9 purification with three elution steps. A) Chromatographic profile of RNAs elution with arginine monolith. Chromatography was carried out at 1 mL/min by increasing NaCl concentration in the stepwise gradient: 0.98 M NaCl in 10 mM Tris-HCl buffer, 1.12 M NaCl in 10 mM Tris-HCl buffer, 1.62 M NaCl in 10 mM Tris-HCl buffer (pH 6.5). B) Polyacrylamide gel electrophoresis of samples collected from chromatographic assay. Fractions from peaks 1, 2 and 3 are represented in lanes 1, 2 and 3 respectively. Lane S represents the RNA sample injected onto the monolith disk.

This chromatographic assay is shown in Figure 21A and it is possible to notice from both lane 1 (Figure 21B) and lane 2 (Figure 21B) a significant loss of pre-miR-9 along the different steps of the gradient. Considering the RNA contaminants removal, the first step was a good option even though the loss of pre-miRNA was a great inconvenient. The contaminants in the last recovered fraction are not very significant as it can be seen in Figure 21B (lane 3). In fact, comparing the present three step assay with the three step assay involving pre-miR-29, it may be stated that in the former much more pre-miR-9 was lost right after the sample injection (Figure 21A, peak 1) as it can be seen in Figure 21B (lane 1). Even though the second elution step was the same in both strategies (Figure 19A, peak 2 and Figure 21A, peak 2), in the pre-mir-9 experiment there was a smaller amount of tRNAs in the pooled sample. This may be due to the higher elution tendency of the tRNAs in the first step of the assay (Figure 21A, peak 1) where a higher NaCl concentration was used (1 M instead of 0.94 M in the pre-miR-29

experiment). Once again, and similarly to the results represented in Figure 19, the recovery of pre-miR-9 was considerably low, even though a very good isolation of the target RNA was obtained. Although this approach may be good, in both works developed by Pereira and coworkers with arginine and agmatine as ligands, the pre-miRNA loss was almost negligible contrarily to the results presented in Figure 21B [90, 91]. The present study (both involving pre-miR-9 and pre-miR-29) demonstrated that the strategy used along with the arginine ligand resulted better than the study previously reported involving agmatine [90]. Even though, it did not exceed the purity degree of the previously reported study involving arginine ligand [91]. Similarly to the above presented chromatographic strategies for pre-miR-29 purification, a stepwise strategy with two elution steps was planned for pre-miR-9 purification in order to improve its recovery and purity.

3.4.2.2. Stepwise pre-miR-9 purification with two elution steps

As it was verified in the first strategy, undesirable pre-miR-9 losses occurred in the first and second steps of the gradients. Analyzing the behavior of these two critical steps, it was hypothesized that the application of one single step would be advantageous in order to increase pre-miR-9 recovery in the last step without compromising the immediate RNA contaminants elution. This assay was then planned as follows: a first cleaning step of 1 M NaCl in 10 mM Tris-HCl buffer and a pre-miRNA elution step with 1.6 M NaCl in 10 mM Tris-HCl buffer.

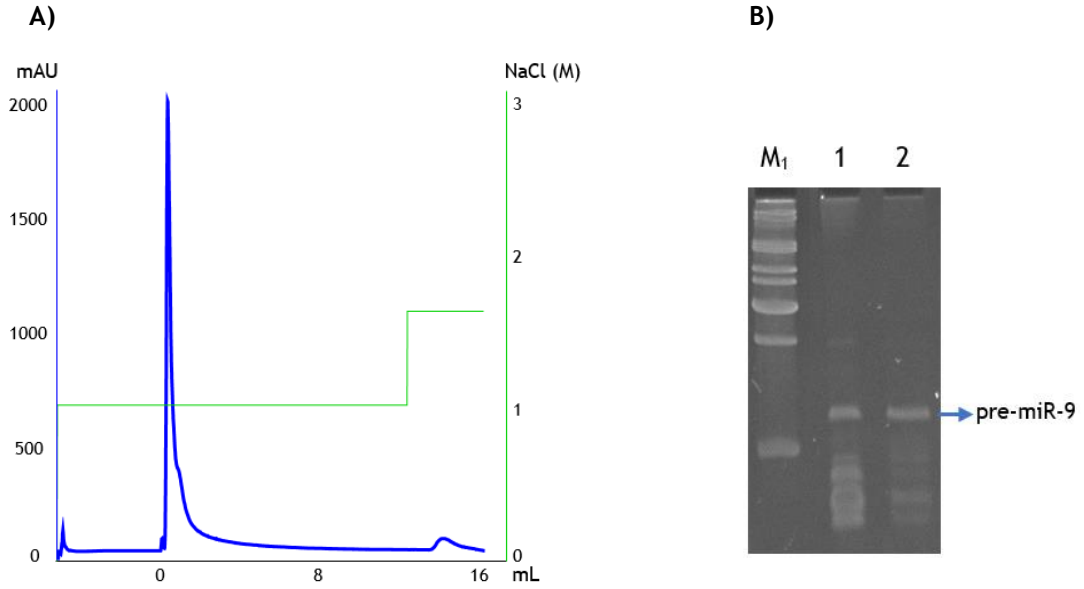

Figure 22 - Stepwise pre-miR-9 purification with two elution steps. A) Chromatographic profile of RNAs elution with arginine monolith. Chromatography was carried out at 1 mL/min by increasing NaCl stepwise gradient: 1 M NaCl in 10 mM Tris-HCl buffer, 1.6 M NaCl in 10 mM Tris-HCl buffer (pH 6.5). B) Polyacrylamide gel electrophoresis of samples collected from chromatographic assay. Fractions from peaks 1 and 2 are represented in lanes 1 and 2 respectively. Lane M1 represents the molecular weight markers of 0.1 to 2 kb.

The first step allowed interactions between pre-miR-9 and the arginine groups of the monolith in a considerable extension as it can be seen by the recovered fraction of peak 2

(Figure 22A) and in lane 2 (Figure 22B). Also in this step, most RNA contaminant species (tRNAs and high weight RNAs like the 5S and 6S) and some pre-miR-9 also eluted, as shown in lane 1 (Figure 22B). In general, arginine ligands distinguished and differentially interacted with various sRNAs molecules, suggesting a specific recognition for the pre-miR-9. This assay resulted better than the three steps experiment because much less pre-miR-9 was lost along the chromatographic experiment and the resulting sample pooled from the second elution step (Figure 22A, peak 2) contained pre-miR-9 in an almost pure condition, as it may be seen in Figure 22B (lane 2). Contrarily to the loss of purity of pre-miR-29 achieved when changing from the three elution steps gradient to the two steps assay, in the case presented in Figure 22 it was verified an increase in the purity degree of pre-miR-9. This assay is comparable to the purification method previously reported by Pereira and coworkers, where the pre-miRNA was recovered in the second gradient step [91]. In Table 1 a summary of the different strategies employed within this work to purify pre-miR-9 and pre-miR-29 as well as its pros and cons is presented. Analyzing Table 1 information, it can be stated that in the present work, among the different purification strategies used for the different pre-miRs, the best strategy for pre-miR-29 purification was the stepwise gradient with three steps and for pre-miR-9 purification the strategy that worked out better was the stepwise gradient with two steps.

Table 1 - Pros and cons of the chromatographic strategies used for pre-miR purification.

	PROS	CONS
pre-miR-29 (0.94 M NaCl, 1.12 M NaCl, 1.6 M NaCl in 10 mM Tris-HCl buffer)	▪ Good purification degree	▪ pre-miR-29 loss in early steps ▪ More salt consuming
pre-miR-29 (1 M NaCl, 1.6 M NaCl in 10 mM Tris-HCl buffer)	▪ Good pre-miR-29 recovery	▪ Low purification degree ▪ Considerable pre-miR-29 loss in early steps
pre-miR-9 (0.98 M NaCl, 1.12 M NaCl, 1.62 M NaCl in 10 mM Tris-HCl buffer)	▪ Good purification degree	▪ pre-miR-9 loss in early steps ▪ More salt consuming
pre-miR-9 (1 M NaCl, 1.6 M NaCl in 10 mM Tris-HCl buffer)	▪ Excellent purification degree	▪ Considerable pre-miR-9 loss in early steps

The strategies used in this study for pre-miRNA purification can be improved in the future in order to achieve minimum product loss. However, the affinity chromatography may be

considered a very good approach to purify these nucleic acid molecules because of the great advantages it presents in comparison to other RNA purification chromatographic strategies namely the hydrophobic or electrostatic chromatography and affinity tags.

As mentioned before, our group has reported several affinity chromatographic studies involving hydrophobic interactions by using $(NH_4)_2SO_4$ stepwise gradient. In hydrophobic chromatography with $(NH_4)_2SO_4$, the elution occurs by decreasing salt concentration in buffer solution [87, 91, 93]. Lysine ligand specifically interacted with one of the interest molecules, the pre-miR-29 and successfully purified it [93]. O-*phospho*-l-tyrosine was also used as ligand under hydrophobic conditions to purify pre-miR-29 with 52% purity [87]. Histidine amino acid has also been used to interact with sRNA and ribosomal RNA (rRNA) and isolated them under hydrophobic conditions [92]. Although these purification methods offer an easy and reproducible way to purify diverse RNA species, especially siRNA, the $(NH_4)_2SO_4$ concentrations used in these chromatographic assays present several environmental impact problems and lead to higher costs than NaCl [18].

The affinity tags-based chromatography is also a reliable and commonly used technique for sRNA purification. Even though the several advantages this approach may present, there are some factors that undervalue this type of chromatography. Among these, there may be pointed the need of several molecules such as the tag itself that has to be added to the RNA, the tag receptor of the chromatographic support and elution molecules including enzymes needed to separate the interest RNA from the tag [100, 101]. All these additional elements rise the probability of procedure complications such as the cleaving reaction that might not always occur as planned, taking longer time periods or even inducing conformational alterations to the interest molecule. Because of this complex methodology and the additional elements, further purification processes may be necessary [18]. Here, once again, the strategy that was explored during this investigation on chromatographic alternatives to isolate specific pre-miRNAs, turns out to be advantageous comparing to tag affinity chromatography because no alterations are made to the target molecule, it is not submitted to denaturing conditions and no enzyme influence is required to elute the RNA. This way, the insertion of undesired molecules that can not be present in samples for therapeutic purposes is avoided, facilitating the whole process. All these factors help to maintain low cost chromatographic purifications reliable and safer.

3.5. Genomic DNA and protein quantification of the purified RNA fractions

The best arginine-affinity monolith strategies were established for both target pre-miRNAs purification, allowing the removal of the majority of the impurities present in the crude RNA fraction. However, as the application of recombinant RNA molecules for therapeutic purposes must follow strict criteria, the levels of contaminants, including proteins and gDNA, in the

purified RNA fractions were assessed to verify the quality of these pre-miRNAs and consequently the success of the used processes. The regulation for the miRNA is not established by the regulatory authorities [86, 102]. Nevertheless, the pDNA products application are already regulated by authorities such as the Food and Drug Administration (FDA), European Agency for the Evaluation of Medical Products (EMEA) and World Health Organization (WHO). In Table 2, the gDNA and the protein limit concentration values are presented. In the present work, the endotoxin presence wasn't evaluated, but it is a very important test for pharmaceutical applications, once these can't be over 10 EU/mg of plasmid (tested with Limulus Amebocyte Lysate (LAL)) [103].

Table 2 - Quantitative analysis of purity of pre-miR-9 and pre-miR-29 isolated by affinity chromatography using arginine monolithic disk. ND stands for "not detected".

Sample	Genomic DNA (ng/uL)	Proteins (uL/mL)
Initial Sample	0.607 ± 0.149	14.817 ± 0.689
Pre-miR-29 (3 steps)	0.091 ± 0.013	ND
Pre-miR-29 (2 steps)	0.056 ± 0.007	ND
Pre-miR-9 (3 steps)	0.206 ± 0.037	ND
Pre-miR-9 (2 steps)	0.268 ± 0.045	ND
Limit values established by regulatory agencies [103, 104]	< 2 µg/mg pDNA (tested with by RT-qPCR)	Undetectable (tested with BCA assay)

As it can be seen in Table 2, the initial RNA sample extracted from *E. coli DH5a* had a protein content of approximately 14.817 µg/mL. During the chromatographic process, as shown in rows 2 to 5 (Table 2), the protein contaminants were eliminated, suggesting that the optimized purification methods are able to remove this contaminant, even improving the previously reported methods [90, 91]. On the other hand, it can be verified by row 1 in Table 2 that the initial sample, along with proteins, was also contaminated with gDNA of *E. coli DH5a*. The chromatographic assay influenced the gDNA content of the final sample. As shown in rows 2 to 5 of Table 2 the gDNA content significantly decreased in comparison to the concentration of the initial sample (around 0.607 ng/µL). Relatively to the pre-miR-29 samples it can be seen in Table 2 that the elimination of DNA contaminants was more successful than in the pre-miR-9 samples. In the pre-miR-29 samples the final gDNA content was less than 0.1 ng/µL and in the pre-miR-9 samples the gDNA content was less than 0.3 ng/µL.

It can be concluded that these purification methods are efficient in the protein removal, and also somehow beneficial in the gDNA removal. A hypothesis that can be posed to explain the difference between the presence of proteins and gDNA is the similarity between the DNA and the RNA molecules that may allow these two nucleic acids to respond to certain conditions similarly.

3.6. BACE 1 and PSEN quantification in CS/pre-miR-9 and CS/pre-miR-29 N2a695 transfected cells

The main goal of this work was to produce recombinant pre-miR-9 and pre-miR-29 using the versatile *E. coli DH5α* and to purify these pre-miRNAs by affinity chromatography aiming their preparation for a possible therapeutic application. Therefore, based in previously reported strategies [96], the effects of the target pre-miRNAs on the levels of BACE1 and PSEN mRNAs were analyzed to hypothesize whether a possible delay on the progression of the AD would be possible hereafter. For this purpose, the N2a695 cell line was chosen because of their ability to express constitutive endogenous human BACE1 [96], which allows experimental procedures involving this protein. In order to transfect the cells and get access to the cytoplasm of the cells where pre-miRNAs are processed as usual, pre-miRNAs were combined with CS polyplexes as they have been previously reported as good delivery systems [75, 78, 79, 105]. These polyplexes have been reported to penetrate the BBB [105], being an asset for this study, as a future prospect. N2a695 cells were transfected with polyplexes of CS loaded with recombinant pre-miR-9 or pre-miR-29 during 72 hours, in order to study the effect of these two RNAs in the expression patterns of specific mRNAs of proteins involved in the amyloidogenic pathway, such as BACE1 and PSEN. Furthermore, it was also performed RT-qPCR for RNA from N2a695 cells transfected with scrambled RNA at 72 hours (Figures 23, 24).

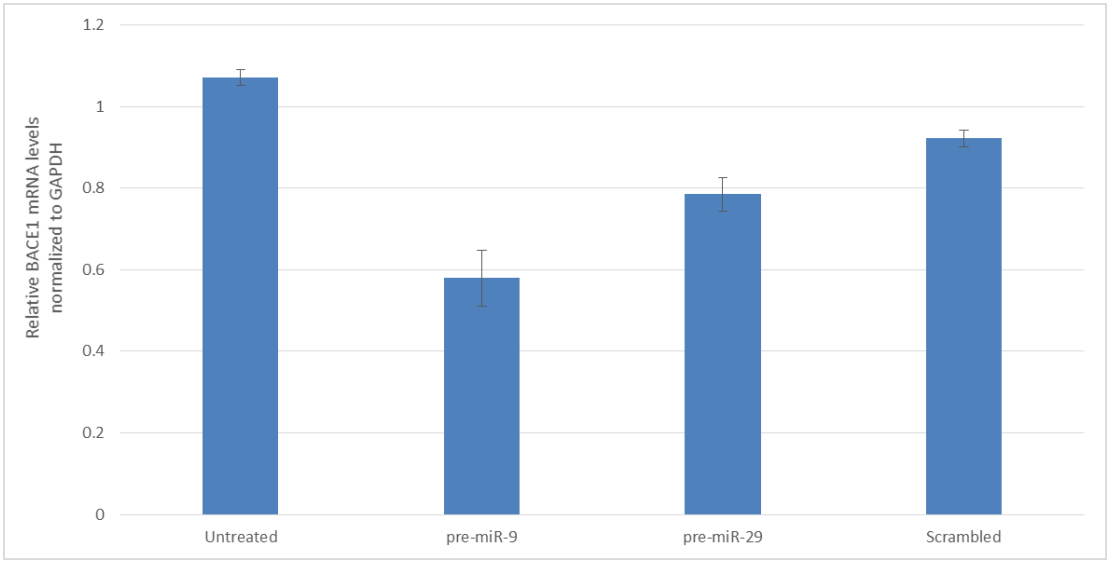

Figure 23 - Effect of pre-miR-9 and pre-miR-29 on the expression pattern of BACE1 mRNA levels in N2a695 cells normalized to GAPDH mRNA. Untreated cells and scrambled are control tests. Results presented are mean of three independent tests each.

As shown in Figure 23, RT-qPCR results revealed that BACE1 mRNA levels in the cells were significantly reduced after treatment with polyplexes-loaded with pre-miR-9 or pre-miR-29 compared to untreated cells and cells transfected with the scrambled RNA. Data analysis showed that CS/pre-miR-29 significantly decreased hBACE1 mRNA expression to ~22 %, while N2a695 cells treated with CS/pre-miR-9 had hBACE1 mRNA decreased by ~42 %, at 72 hours of transfection, comparing to untreated cells (Figure 23). It is observed a significant difference between the BACE1 mRNA levels in cells treated with pre-miR-9 and cells treated with pre-miR-29. The cells treated with pre-miR-9 had BACE1 mRNA content much lower than cells treated with pre-miR-29, suggesting that the pre-miR-9 is a BACE1 mRNA translation repressor more efficient than the pre-miR-99. The effect of recombinant pre-miR-29 produced by *Rhodovulum sulfidophilum (R. sulfidophilum)* DSM 1374 on the BACE1 mRNA translation had already been studied by Pereira and coworkers [96]. In their work, the CS polyplexes were also used as a delivery system, allowing a good comparison with the present study. It can be said that in the present work the effects of pre-miR-29 in BACE1 mRNA amount were not as sharp as the results reported before. In the previous work the percentage of inhibition was around 78% [96] whereas in the present work the inhibition percentage was around 22%. The discrepancy between these results may have different causes. A possible cause for this reduced pre-miR-29 efficiency is its degradation somewhere between the purification process and the transfection of N2a695 cells. The RNA is an extremely vulnerable molecule and slight temperature variations are enough to alter the pre-miR-29 molecular structure. Another possible explanation for this situation is the possible lower transfection efficiency. If a problem occurred either with the nanoparticles or along the cell line transfection with pre-miR-29, the reduced miR-29 levels within the cells wouldn't be enough to inhibit the target mRNAs in a good extension.

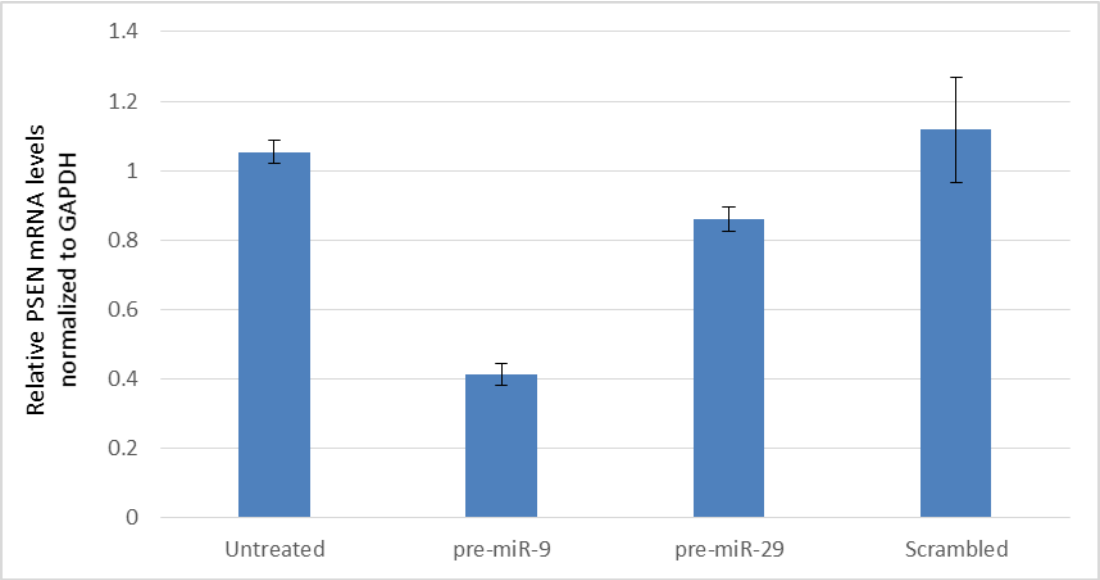

Figure 24 - Effect of pre-miR-9 and pre-miR-29 on the expression pattern of PSEN mRNA levels in N2a695 cells normalized to GAPDH mRNA. Untreated cells and scrambled are control tests. Results presented are mean of three independent tests each.

Following the evaluation of the effect of the transfection of N2a695 cells with polyplexes loaded with recombinant pre-miR-9 or pre-miR-29 on BACE1 mRNA levels, it was also evaluated its effect on PSEN mRNA levels by RT-qPCR measurements. It was already known that BACE1 and PSEN mRNA are targets for the miR-9 and that it is downregulated in AD brains [64, 106] and this is what inspired this study along the previous work developed by our group specifically involving pre-miR-29 [96]. The pattern of Figure 24 is similar to the results presented in Figure 23. Both pre-miR-9 and pre-miR-29 led to a decrease of PSEN mRNA levels. The PSEN mRNA levels of the treated cells were lower comparing to the untreated cells. Similarly, to the effects caused in the BACE1 mRNA translation, also the PSEN mRNA translation was repressed in more extension by the action of pre-miR-9 than by the action of pre-miR-29. The PSEN mRNA levels were decreased by approximately 14 % in cells transfected with CS/pre-miR-29, and by 59 % in those transfected by CS/pre-miR-9 complexes, comparing to untreated cells (Figure 24). It is also verified that the lower inhibition of BACE1 mRNA by pre-miR-29 already verified in Figure 23 was even lower when applied to the PSEN mRNA bearing 14% of inhibition, suggesting higher specificity to the BACE1 mRNA than to the PSEN mRNA. Comparing these two graphics presented above (Figure 23 and 24), it can be concluded that both pre-miR-9 and pre-miR-29 had the expected activity, being able to reduce the levels of BACE1 and PSEN mRNAs, which consequently, could led to a decrease of these proteins expression. Also, it can be concluded that pre-miR-9 has a stronger mRNA translation repression effect of these two mRNAs than pre-miR-29. The cells transfected with scrambled RNA presented a higher PSEN mRNA content, however, the amplitude of the interval of values was also wider suggesting that these scrambled results are less reliable than the scrambled results of the experiments involving the BACE1 mRNA. Since the N2a695 treatment with each nucleic acid would result in the reduction of the level of the proteins involved in the amyloid

plaque formation, it is possible that the cell transfection with both pre-miRNAs would result in a synergic effect of BACE1 and PSEN mRNAs translation repression avoiding the high rate of amyloid plaque formation in a situation involving animal models.

Chapter IV

Conclusions and Future Perspectives

AD is a worldwide spread problem especially among the elderly that currently has no known cure. Anyway, different pathways involved in the evolution of this disease have been significantly studied and characterized. For this matter, the evolution on the field may lead to the development of molecules capable of reverting the main causes of this disease. The miRNAs have been extensively investigated and are potential therapeutic molecules since they intervene in protein translation. This is a very exploitable property because it allows the external manipulation of specific pathways with a certain objective. miR-9 and mi-29 have been related with the AD, specifically by influencing the expression levels of BACE1 and PSEN proteins. BACE1 and PSEN are respectively an APP cleaving enzyme and a protein necessary to the correct operation of the APP cleaving γ-secretase enzyme. The highly specific BACE1 translation repression by the action of miR-29 is well known as well as the PSEN translation repression by miR-9. The action of the pre-miR-29 in N2a695 (cells that express the APP 695) was previously studied by our group. In the present work the effect of the miR-9 and miR-29 was studied in the same cell line.

miR-9 and miR-29 were produced by recombinant *E. coli DH5a* transformed with the pBHSR1-RM plasmid. The previously reported optimal growth conditions for the *E. coli DH5a* were applied in this situation and it was verified that this microorganism is able to proliferate until 6 hours after the fermentation initiation. In particular, the highest expression levels of the target RNAs were achieved at 6 hours of fermentation. Similarly, the protein concentration achieved the higher values after 5 hours of fermentation. On the other hand, the gDNA content along the fermentation time suffered a decrease between 1 and 6 hours, after which an increase was observed. This could be due to the release of intracellular components of *E. coli DH5a*. It is important to reinforce that the recombinant small-scale production presents benefits comparing to the chemical or the *in vitro* nucleic acid production. The recombinant production is a more simple, cost-effective and accurate process, allowing the production of small or longer molecules and safer purification methods can be used to isolate the target molecule from a mixture.

After establishing appropriate upstream strategies for obtaining the recombinant RNA of interest, the next step carried out within this project was the development of a suitable recovery and purification process with an arginine monolithic support. The well-established phenol-chlorophorm method was applied for RNA extraction and allowed the recovery of intact and stable RNA fractions. For the purification process, the arginine monolith support was chosen because of the interesting affinity interactions it can establish with several

molecules. Extracted samples were injected into the support and interacted immediately with the arginine affinity ligands of the stationary phase. Two stepwise NaCl gradients (a stepwise gradient with three elution steps and a stepwise gradient with two steps) were used to elute different RNA species. The best purification strategy for pre-miR-29 purification was the stepwise gradient with three steps (0.94 M NaCl, 1.12 M NaCl, 1.6 M NaCl in 10 mM Tris-HCl buffer at pH 6.5). The pre-miR-9 purification was more successful when the stepwise gradient with two steps was applied (1 M NaCl, 1.6 M NaCl in 10 mM Tris-HCl buffer at pH 6.5). The purified nucleic acids samples were analyzed to verify the presence of proteins or gDNA. Noteworthy there were no protein species in the collected samples. The gDNA content was significantly reduced, in comparison to the initial sample. This affinity chromatography turned out as a good miRNA isolation method even though some efforts could be made in order to improve the final miRNA recovery. Therefore, some competition agents could be used in the mobile phase trying to achieve higher selectivity towards pre-miRNAs. For example, arginine competition studies could be carried out to achieve higher specificity also combining with an optimization of different parameters like pH, temperature and salt concentration.

To verify whether the pre-miR-9 and pre-miR-29 mature forms actually have a repressive effect on the translation of the amyloidogenic BACE1 and PSEN proteins' mRNA, a cell line that overexpresses the BACE1 was chosen to be transfected with these pre-miRNAs and carry out the studies, the N2a695 cell line. This cell line was transfected with CS nanoparticles containing pre-miR-9 and pre-miR-29. A decrease on BACE1 and PSEN mRNAs levels in transfected N2A 695 cells was verified either for pre-miR-9 or pre-miR-29 transfected cells. The miR-29 induced a repression of ~22 % in BACE1 mRNA levels and ~42 % in PSEN mRNA. On the other hand, the miR-9 had ~14 % inhibitory effect on BACE1 mRNA levels and ~59 % inhibitory effect on PSEN mRNA. Nevertheless, the effect caused by miR-29 was not as extensive as previously reported by our group, in which the BACE1 mRNA translation inhibition was around 78 % [96]. These results may have been due to several reasons such as pre-miR-29 committed biological conformation or N2a695 cell line transfection failures. To overcome these problems additional care must be taken when manipulating the RNA species, since they are vulnerable to environmental conditions. The pre-miRNA delivery systems may also be further studied and developed to improve the efficacy of the method. For example, some polymers can be explored such as the Polyethylenimine (PEI) or Poly(lactic-co-glycolic acid (PLGA), or even the conjugation between CS and the latest polymers mentioned.

This study could be further deepen by evaluating the possible synergy between pre-miR-9 and pre-miR-29. This could be assessed by transfecting cell lines with both RNAs together and experiences on the effects of combined differential concentrations could be carried out. Also, transfection studies with larger time periods could be done to understand if there is no toxic

effect caused by the interest pre-miRNAs. More investigation could also be done by exploring other techniques such as Western Blot or Immunofluorescence with BACE1 and PSEN.

As mentioned before, it would be important to run tests in animal models to access the acceptance of these nucleic acids by the living organisms and if the effects *in vivo* are still as promising and safe as in these preliminary *in vitro* studies. In this matter the parameters established by Food and Drug Administration (FDA) have to be taken into account when analyzing the integrity, biological activity and purity of the pre-miRNAs aimed to be used as biotherapeutics.

Chapter V

References

1. Bartel, D.P.: MicroRNAs: genomics, biogenesis, mechanism, and function. Cell. 116, 281–97 (2004).
2. Graves, P., Zeng, Y.: Biogenesis of Mammalian MicroRNAs: A Global View. Genomics, Proteomics Bioinforma. 10, 239–245 (2012).
3. Kim, V.N.: MicroRNA precursors in motion: exportin-5 mediates their nuclear export. Trends Cell Biol. 14, 156–159 (2004).
4. Lund, E.: Nuclear Export of MicroRNA Precursors. Science. 303, 95–98 (2004).
5. Lee, R.C.: The C . elegans Heterochronic Gene lin-4 Encodes Small RNAs with Antisense Complementarity to & II-14. 75, 843–854 (1993).
6. Tétreault, N., De Guire, V.: MiRNAs: Their discovery, biogenesis and mechanism of action. Clin. Biochem. 46, 842–845 (2013).
7. Zeng, Y., Yi, R., Cullen, B.R.: Recognition and cleavage of primary microRNA precursors by the nuclear processing enzyme Drosha. EMBO J. 24, 138–148 (2005).
8. Zeng, Y.: Principles of micro-RNA production and maturation. Oncogene. 25, 6156–6162 (2006).
9. Melo, C.A., Melo, S.A.: Non-coding RNAs and Cancer. Non-coding RNAs Cancer. 5–25 (2014).
10. Martin, E.C., Qureshi, A.T., Dasa, V., Freitas, M.A., Gimble, J.M., Davis, T.A.: MicroRNA regulation of stem cell differentiation and diseases of the bone and adipose tissue: Perspectives on miRNA biogenesis and cellular transcriptome. Biochimie. (2015).
11. Savagner, F., Le Pennec, S., Rivalin, R., Eyer, J.: Les microARNs. Rev. Francoph. des Lab. 49–54 (2015).
12. Rodriguez, A.: Identification of Mammalian microRNA Host Genes and Transcription Units. Genome Res. 14, 1902–1910 (2004).
13. Treiber, T., Treiber, N., Meister, G.: Regulation of microRNA biogenesis and function. Thromb. Haemost. 107, 605–610 (2012).
14. Lenkala, D., Gamazon, E.R., LaCroix, B., Im, H.K., Huang, R.S.: MicroRNA biogenesis and cellular proliferation. Transl. Res. 166, 145–151 (2015).
15. Lee, Y., Kim, M., Han, J., Yeom, K.-H., Lee, S., Baek, S.H., Kim, V.N.: MicroRNA genes are transcribed by RNA polymerase II. EMBO J. 23, 4051–4060 (2004).
16. Saini, H.K., Enright, A.J., Griffiths-Jones, S.: Annotation of mammalian primary microRNAs. BMC Genomics. 9, (2008).
17. Cai, X., Hagedorn, C.H., Cullen, B.R.: Human microRNAs are processed from capped, polyadenylated transcripts that can also function as mRNAs. RNA. 10, 1957–1966

(2004).
18. Pereira, P., Queiroz, J.A., Figueiras, A., Sousa, F.: Affinity approaches in RNAi-based therapeutics purification. J. Chromatogr. B. 1–12 (2016).
19. Han, J., Lee, Y., Yeom, K.H., Nam, J.W., Heo, I., Rhee, J.K., Sohn, S.Y., Cho, Y., Zhang, B.T., Kim, V.N.: Molecular Basis for the Recognition of Primary microRNAs by the Drosha-DGCR8 Complex. Cell. 125, 887–901 (2006).
20. Filipowicz, W., Jaskiewicz, L., Kolb, F. a., Pillai, R.S.: Post-transcriptional gene silencing by siRNAs and miRNAs. Curr. Opin. Struct. Biol. 15, 331–341 (2005).
21. Schonrock, N., Götz, J.: Decoding the non-coding RNAs in Alzheimer's disease. Cell. Mol. Life Sci. 69, 3543–3559 (2012).
22. Zeng, Y.: Structural requirements for pre-microRNA binding and nuclear export by Exportin 5. Nucleic Acids Res. 32, 4776–4785 (2004).
23. Yi, R., Qin, Y., Macara, I.G., Cullen, B.R.: Exportin-5 mediates the nuclear export of pre-microRNAs and short hairpin RNAs. Genes Dev. 17, 3011–3016 (2003).
24. Bohnsack, M.T., Czaplinski, K., Gorlich, D.: Exportin 5 is a RanGTP-dependent dsRNA-binding protein that mediates nuclear export of pre-miRNAs. Cold Spring Harb. Lab. Press. 10, 185–91 (2004).
25. Wahid, F., Shehzad, A., Khan, T., Kim, Y.Y.: MicroRNAs: Synthesis, mechanism, function, and recent clinical trials. Biochim. Biophys. Acta - Mol. Cell Res. 1803, 1231–1243 (2010).
26. Katahira, J., Yoneda, Y.: Nucleocytoplasmic transport of MicroRNAs and related small RNAs. Traffic. 12, 1468–1474 (2011).
27. Murphy, D., Dancis, B., Brown, J.R.: The evolution of core proteins involved in microRNA biogenesis. BMC Evol Biol. 8, 1–18 (2008).
28. Blahna, M.T., Hata, A.: Regulation of miRNA biogenesis as an integrated component of growth factor signaling. Curr. Opin. Cell Biol. 25, 233–240 (2013).
29. Ma, J.-B., Ye, K., Patel, D.J.: Structural basis for overhang-specific small interfering RNA recognition by the PAZ domain. Nature. 429, 318–322 (2004).
30. Zhang, H., Kolb, F.A., Jaskiewicz, L., Westhof, E., Filipowicz, W.: Single processing center models for human Dicer and bacterial RNase III. Cell. 118, 57–68 (2004).
31. Jin, P., Alisch, R.S., Warren, S.T.: RNA and microRNAs in fragile X mental retardation. Nat. Cell Biol. 6, 1048–1053 (2004).
32. Liu, J., Rivas, F. V, Wohlschlegel, J., Yates, J.R., Parker, R., Hannon, G.J.: A role for the P-body component GW182 in microRNA function. Nat. Cell Biol. 7, 1261–1266 (2005).
33. Chu, C.Y., Rana, T.M.: Translation repression in human cells by MicroRNA-induced gene silencing requires RCK/p54. PLoS Biol. 4, 1122–1136 (2006).
34. Frank, F., Sonenberg, N., Nagar, B.: Structural basis for 5′-nucleotide base-specific recognition of guide RNA by human AGO2. Nature. 465, 818–822 (2010).
35. Pasquinelli, A.E., Reinhart, B.J., Slack, F., Martindale, M.Q., Kuroda, M.I., Maller, B.,

Hayward, D.C., Ball, E.E., Degnan, B., Müller, P., Spring, J., Srinivasan, A., Fishman, M., Finnerty, J., Corbo, J., Levine, M., Leahy, P., Davidson, E., Ruvkun, G.: Conservation of the sequence and temporal expression of let-7 heterochronic regulatory RNA. Nature. 408, 86–89 (2000).

36. Ho, P.Y., Yu, A.M.: Bioengineering of noncoding RNAs for research agents and therapeutics. Wiley Interdiscip. Rev. RNA. 7, 186–197 (2016).
37. Vasudevan, S.: Posttranscriptional Upregulation by MicroRNAs. Wiley Interdiscip. Rev. RNA. 3, 311–330 (2012).
38. Bartel, D.P.: MicroRNAs: target recognition and regulatory functions. Cell. 136, 215–33 (2009).
39. Satoh, J.: Molecular network of microRNA targets in Alzheimer's disease brains. Exp. Neurol. 235, 436–446 (2012).
40. Hardy, J.: Amyloid, the presenilins and Alzheimer's disease. Trends Neurosci. 20, 154–159 (1997).
41. Bettens, K., Sleegers, K., Van Broeckhoven, C.: Genetic insights in Alzheimer's disease. Lancet Neurol. 12, 92–104 (2013).
42. Kovacs, D.M., Gersbacher, M.T., Kim, D.Y.: Alzheimer's secretases regulate voltage-gated sodium channels. Neurosci. Lett. 486, 68–72 (2010).
43. Stelzmann, R.A., Schnitzlein, H.N., Murtagh, F.R.: An English translation of Alzheimer's 1907 paper, "uber eine eigenartige erkankung der hirnrinde." Clin. Anat. 8, 429–431 (1995).
44. Götz, J., Matamales, M., Götz, N.N., Ittner, L.M., Eckert, A.: Alzheimer's disease models and functional genomics-How many needles are there in the haystack? Front. Physiol. 3, (2012).
45. Reddy, P.H., Tonk, S., Kumar, S., Vijayan, M., Kandimalla, R., Kuruva, C.S., Reddy, A.P.: A critical evaluation of neuroprotective and neurodegenerative MicroRNAs in Alzheimer's disease. Biochem. Biophys. Res. Commun. 1–10 (2016).
46. Piaceri, I., Nacmias, B., Sorbi, S., Naemias, B.: Genetics of familial and sporadic Alzheimer's disease. Front. Biosci. 5, 167–177 (2013).
47. Selkoe, D.J.: Alzheimer's disease results from the cerebral accumulation and cytotoxicity of amyloid beta-protein. J Alzheimers Dis. 3, 75–80 (2001).
48. Barbato, C., Ruberti, F., Cogoni, C.: Searching for MIND: MicroRNAs in Neurodegenerative Diseases. J. Biomed. Biotechnol. 2009, 1–8 (2009).
49. Bursavich, M.G., Harrison, B.A., Blain, J.-F.: Gamma Secretase Modulators: New Alzheimer's Drugs on the Horizon? J. Med. Chem. acs.jmedchem. (2016).
50. Gralle, M., Ferreira, S.T.: Structure and functions of the human amyloid precursor protein: The whole is more than the sum of its parts. Prog. Neurobiol. 82, 11–32 (2007).
51. Turner, P.R., O'Connor, K., Tate, W.P., Abraham, W.C.: Roles of amyloid precursor protein and its fragments in regulating neural activity, plasticity and memory. (2003).

52. Chapman, P.F., Falinska, a M., Knevett, S.G., Ramsay, M.F.: Genes, models and Alzheimer's disease. Trends Genet. 17, 254–261 (2001).
53. Evin, G., Weidemann, A.: Biogenesis and metabolism of Alzheimer's disease Abeta amyloid peptides. Peptides. 23, 1285–1297 (2002).
54. Rossor, M.N.: Molecular pathology of Alzheimer's disease. J. Neurol. Neurosurg. Psychiatry. 56, 583–586 (1993).
55. Vassar, R., Kovacs, D.M., Yan, R., Wong, P.C.: The -Secretase Enzyme BACE in Health and Alzheimer's Disease: Regulation, Cell Biology, Function, and Therapeutic Potential. J. Neurosci. 29, 12787–12794 (2009).
56. Lichtenthaler, S.F., Wang, R., Grimm, H., Uljon, S.N., Masters, C.L., Beyreuther, K.: Mechanism of the cleavage specificity of Alzheimer's disease gamma-secretase identified by phenylalanine-scanning mutagenesis of the transmembrane domain of the amyloid precursor protein. Proc. Natl. Acad. Sci. U. S. A. 96, 3053–3058 (1999).
57. Fukumoto: ß-Secretase Protein and Activity Are Increased in the Neocortex in Alzheimer Disease—Correction. Arch. Neurol. 59, 1381–1389 (2002).
58. Spies, P.E., Verbeek, M.M., van Groen, T., Claassen, J.A.H.R.: Reviewing reasons for the decreased CSF Abeta42 concentration in Alzheimer disease. Front. Biosci. (Landmark Ed. 17, 2024–2034 (2012).
59. Selkoe, D.J., Wolfe, M.S.: Presenilin: Running with Scissors in the Membrane. Cell. 131, 215–221 (2007).
60. Edbauer, D., Winkler, E., Regula, J.T., Pesold, B., Steiner, H., Haass, C.: Reconstitution of gamma-secretase activity. Nat. Cell Biol. 5, 486–8 (2003).
61. Schonrock, N., Matamales, M., Ittner, L.M., Götz, J.: MicroRNA networks surrounding APP and amyloid-ß metabolism — Implications for Alzheimer's disease. Exp. Neurol. 235, 447–454 (2012).
62. Delay, C., Mandemakers, W., Hébert, S.S.: MicroRNAs in Alzheimer's disease. Neurobiol. Dis. 46, 285–290 (2012).
63. Czech, C., Tremp, G., Pradier, L.: Presenilins and Alzheimer's disease: Biological functions and pathogenic mechanisms, (2000).
64. Hébert, S.S., Horré, K., Nicolaï, L., Papadopoulou, A.S., Mandemakers, W., Silahtaroglu, A.N., Kauppinen, S., Delacourte, A., De Strooper, B.: Loss of microRNA cluster miR-29a/b-1 in sporadic Alzheimer's disease correlates with increased BACE1/beta-secretase expression. Proc. Natl. Acad. Sci. U. S. A. 105, 6415–6420 (2008).
65. Lei, X., Lei, L., Zhang, Z., Zhang, Z., Cheng, Y.: Downregulated miR-29c correlates with increased BACE1 expression in sporadic Alzheimer's disease. Int. J. Clin. Exp. Pathol. 8, 1565–1574 (2015).
66. Lukiw, W.J., Andreeva, T. V., Grigorenko, A.P., Rogaev, E.I.: Studying micro RNA function and dysfunction in Alzheimer's disease. Front. Genet. 3, 1–13 (2013).
67. Delay, C., Hébert, S.S.: MicroRNAs and Alzheimer's Disease Mouse Models: Current

Insights and Future Research Avenues. Int. J. Alzheimers. Dis. 2011, 1–7 (2011).
68. Chen, X., Zhu, L., Ma, Z., Sun, G., Luo, X., Li, M., Zhai, S., Li, P., Wang, X.: Oncogenic miR-9 is a target of erlotinib in NSCLCs. Sci Rep. 5, 1–11 (2015).
69. Tan, L., Yu, J.-T., Hu, N., Tan, L.: Non-coding RNAs in Alzheimer's Disease. Mol. Neurobiol. 47, 382–393 (2013).
70. Geekiyanage, H., Chan, C.: MicroRNA-137/181c Regulates Serine Palmitoyltransferase and In Turn Amyloid , Novel Targets in Sporadic Alzheimer's Disease. J. Neurosci. 31, 14820–14830 (2011).
71. Zong, Y., Wang, H., Dong, W., Quan, X., Zhu, H., Xu, Y., Huang, L., Ma, C., Qin, C.: miR-29c regulates BACE1 protein expression. Brain Res. 1395, 108–115 (2011).
72. Holohan, K.N., Lahiri, D.K., Schneider, B.P., Foroud, T., Saykin, A.J.: Functional microRNAs in Alzheimer's disease and cancer: Differential regulation of common mechanisms and pathways. Front. Genet. 3, 1–16 (2013).
73. Junn, E., Mouradian, M.M.: MicroRNAs in neurodegenerative diseases and their therapeutic potential. Pharmacol. Ther. 133, 142–150 (2011).
74. Roshan, R., Ghosh, T., Scaria, V., Pillai, B.: MicroRNAs: novel therapeutic targets in neurodegenerative diseases. Drug Discov. Today. 14, 1123–1129 (2009).
75. Saraiva, C., Praça, C., Ferreira, R., Santos, T., Ferreira, L., Bernardino, L.: Nanoparticle-mediated brain drug delivery: Overcoming blood-brain barrier to treat neurodegenerative diseases. J. Control. Release. 235, 34–47 (2016).
76. Burnett, J., Rossi, J.: RNA-based therapeutics: current progress and future prospects. Chem. Biol. 19, 60–71 (2012).
77. Wohlfart, S., Gelperina, S., Kreuter, J.: Transport of drugs across the blood-brain barrier by nanoparticles. J. Control. Release. 161, 264–273 (2012).
78. Katas, H., Alpar, H.O.: Development and characterisation of chitosan nanoparticles for siRNA delivery. J. Control. Release. 115, 216–225 (2006).
79. Pereira, P., Jorge, A.F., Martins, R., Pais, A.A.C.C., Sousa, F., Figueiras, A.: Characterization of polyplexes involving small RNA. J. Colloid Interface Sci. 387, 84–94 (2012).
80. Pereira, P., Pedro, A.Q., Tomás, J., Maia, C.J., Queiroz, J.A., Figueiras, A., Sousa, F.: Advances in time course extracellular production of human pre-miR-29b from Rhodovulum sulfidophilum. Appl. Microbiol. Biotechnol. 100, 3723–3734 (2016).
81. Shiba, Y., Masuda, H., Watanabe, N., Ego, T., Takagaki, K., Ishiyama, K., Ohgi, T., Yano, J.: Chemical synthesis of a very long oligoribonucleotide with 2-cyanoethoxymethyl (CEM) as the 2'-O-protecting group: Structural identification and biological activity of a synthetic 110mer precursor-microRNA candidate. Nucleic Acids Res. 35, 3287–3296 (2007).
82. Ponchon, L., Dardel, F.: Large scale expression and purification of recombinant RNA in Escherichia coli. Methods. 54, 267–273 (2011).
83. Ponchon, L., Dardel, F.: Recombinant RNA technology: the tRNA scaffold. Nat.

Methods. 4, 571–576 (2007).
84. Ponchon, L., Beauvais, G., Nonin-Lecomte, S., Dardel, F.: A generic protocol for the expression and purification of recombinant proteins in Escherichia coli using a combinatorial His6-maltose binding protein fusion tag. Nat. Protoc. 4, 947–959 (2007).
85. Li, M.-M., Addepalli, B., Tu, M.-J., Chen, Q.-X., Wang, W.-P., Limbach, P. a, Lasalle, J.M., Zeng, S., Huang, M., Yu, A.-M.: Chimeric miR-1291 biosynthesized efficiently in E. coli is effective to reduce target gene expression in human carcinoma cells and improve chemosensitivity. Drug Metab Dispos. 43, 1129–1136 (2015).
86. Martins, R., Queiroz, J. a., Sousa, F.: Ribonucleic acid purification. J. Chromatogr. A. 1355, 1–14 (2014).
87. Afonso, A., Pereira, P., Queiroz, J. a., Sousa, Â., Sousa, F.: Purification of pre-miR-29 by a new O-phospho-l-tyrosine affinity chromatographic strategy optimized using design of experiments. J. Chromatogr. A. 1343, 119–127 (2014).
88. Sousa, F., Cruz, C., Queiroz, J.A.: Amino acids-nucleotides biomolecular recognition: From biological occurrence to affinity chromatography. J. Mol. Recognit. 23, 505–518 (2010).
89. M. Peck, E., D. Smith, B.: Synthetic Receptors for Biomolecules. (2015).
90. Pereira, P., Sousa, A., Queiroz, J. a, Figueiras, A., Sousa, F.: Pharmaceutical-grade pre-miR-29 purification using an agmatine monolithic support. J. Chromatogr. A. 1368, 173–182 (2014).
91. Pereira, P., Sousa, Â., Queiroz, J., Correia, I., Figueiras, A., Sousa, F.: Purification of pre-miR-29 by arginine-affinity chromatography. J. Chromatogr. B. 951–952, 16–23 (2014).
92. Martins, R., Queiroz, J.A., Sousa, F.: Histidine affinity chromatography-based methodology for the simultaneous isolation of Escherichia coli small and ribosomal RNA. Biomed. Chromatogr. 26, 781–788 (2011).
93. Pereira, P., Sousa, Â., Queiroz, J., Figueiras, A., Sousa, F.: New approach for purification of pre-miR-29 using lysine-affinity chromatography. J. Chromatogr. A. 1331, 129–132 (2014).
94. Martins, R., Maia, C.J., Queiroz, J. a, Sousa, F.: A new strategy for RNA isolation from eukaryotic cells using arginine affinity chromatography. J. Sep. Sci. 35, 3217–3226 (2012).
95. Chomczynski, P., Sacchi, N.: The single-step method of RNA isolation by acid guanidinium thiocyanate – phenol – chloroform extraction : twenty-something years on. Nat. Protoc. 1, 581–585 (2006).
96. Pereira, P.A., Tomás, J.F., Queiroz, J.A., Figueiras, A.R., Sousa, F.: Recombinant pre-miR-29b for Alzheimer´s disease therapeutics. Sci. Rep. 6, 1–11 (2016).
97. Li, M., Wang, W., Wu, W., Huang, M., Yu, A.: Rapid Production of Novel Pre-MicroRNA Agent hsa-mir-27b in Escherichia coli Using Recombinant RNA Technology for Functional Studies in Mammalian Cells. 42, 1791–1795 (2014).

98. Gopal, G.J., Kumar, A.: Strategies for the production of recombinant protein in Escherichia coli. Protein J. 32, 419–25 (2013).
99. Farrell, R.E.: RNA Methodologies: Laboratory Guide for Isolation and Characterization. (2010).
100. Srisawat, C., Engelke, D.R.: Streptavidin aptamers: affinity tags for the study of RNAs and ribonucleoproteins. RNA. 7, 632–641 (2001).
101. Ørom, U.A., Lund, A.H.: Isolation of microRNA targets using biotinylated synthetic microRNAs. Methods. 43, 162–165 (2007).
102. McGinnis, A.C., Chen, B., Bartlett, M.G.: Chromatographic methods for the determination of therapeutic oligonucleotides. J. Chromatogr. B Anal. Technol. Biomed. Life Sci. 883–884, 76–94 (2012).
103. Sousa, A., Sousa, F., Queiroz, J.A.: Differential interactions of plasmid DNA, RNA and genomic DNA with amino acid-based affinity matrices. J. Sep. Sci. 33, 2610–2618 (2010).
104. Sousa, F., Prazeres, D., Queiroz, J.: Improvement of transfection efficiency by using supercoiled plasmid DNA purified with arginine affinity chromatography. J. Gene Med. 11, 79–88 (2009).
105. Sarvaiya, J., Agrawal, Y.K.: Chitosan as a suitable nanocarrier material for anti-Alzheimer drug delivery. Int. J. Biol. Macromol. 72, 454–465 (2015).
106. Yuva-Aydemir, Y., Simkin, A., Gascon, E., Gao, F.-B.: MicroRNA-9. RNA Biol. 8, 557–564 (2011).